TRANSNUCLEAR
AN AREVA COMPANY

May 9, 2013
E-35275

U. S. Nuclear Regulatory Commission
Attn: Document Control Desk
One White Flint North
11555 Rockville Pike
Rockville, MD 20852

Subject: Revision 7 to Transnuclear, Inc. (TN) Application for Amendment 3 to Standardized Advanced NUHOMS® Certificate of Compliance No. 1029, Response to Request for Additional Information (Docket No. 72-1029; TAC No. L24607)

References: Letter from Steve Ruffin (NRC) to Don Shaw (TN), "Second Request for Additional Information for Review of Amendment No. 3 to the Standardized Advanced NUHOMS® Certificate of Compliance No. 1029," April 9, 2013, Docket No.: 72-1029, TAC No.: L24607

This submittal provides responses to the second request for additional information (RAI) forwarded by the letter referenced above. Enclosure 1 herein provides each of the RAI items followed by a TN response. Enclosure 2 provides a list of updated final safety analysis report (UFSAR) new and changed pages, with an indication of which RAI caused the changes. Enclosure 3 provides the new and changed UFSAR pages. In the UFSAR, the pages are annotated as Revision 7, with changes indicated by italicized text and revision bars. New changes are shaded, to distinguish them from previous Amendment 3 changes.

Should the NRC staff require additional information to support review of this application, please do not hesitate to contact Mr. Don Shaw at 410-910-6878 or me at 410-910-6820.

Sincerely,

Kathy M. Nevis (delegate for Paul Triska)

Paul Triska
Vice President, Operations

cc: Steve Ruffin (NRC SFST) as follows:

- Two paper copies of this cover letter and Enclosures 1, 2, and 3
- Two computer disks, each containing this cover letter and Enclosures 1, 2, and 3

7135 Minstrel Way, Suite 300, Columbia, MD 21045
Phone: 410-910-6900 ◆ Fax: 410-910-6902

NMSS

Enclosures:

1. RAIs and Responses
2. List of Changed and New UFSAR Pages, with Associated RAIs
3. Changed and New UFSAR Pages

## CHAPTER 4 – THERMAL EVALUATION

4-1 Clarify how uncertainty in the DSC temperature distribution is factored into the determination of the discretization error described in the response to RAI 4-14.

Section B.4.6.7.1 of FSAR Revision 3 describes the method and calculations to obtain the discretization error for the bounding normal storage condition. However, the obtained results do not appear to include the uncertainty in the applied DSC temperature distribution used in the calculations. The determination of the grid convergence index (GCI) should include this uncertainty. The applicant's approach to determine the DSC temperature distribution does not appear to be adequate to perform GCI calculations because the horizontal storage module (HSM) thermal model does not model internal air circulation explicitly. The applicant's GCI studies also show an increase in the predicted peak cladding temperature, as the mesh is refined. This also supports the belief that the uncertainty in the DSC temperature distribution should be obtained as well to verify the adequacy of the applicant's approach.

This information is needed to determine compliance with 10 CFR 72.236.

### RESPONSE TO RAI 4-1

As noted in response to previous request for additional information, RAI 4-5, the AHSM-HS evaluated in the UFSAR, Section B.4.4 is similar in geometry and dimensions to the HSM-H described in the UFSARs for the Standardized NUHOMS® system (CoC 1004) [1] and NUHOMS® HD system (CoC 1030) [3]. The methodology to calculate the DSC shell temperature profile, as a part of the overall methodology for the evaluation of the thermal performance of HSM-H, was validated using a series of tests on a full-scale mockup of the HSM-H. As described in Section 4.9 of the SER for CoC 1030, Amendment 0 [4], the test protocols were reviewed by NRC and concluded that the methodology predicts conservative temperatures for the system components.

In addition, a comprehensive confirmatory analysis was performed by the NRC in review of CoC 1004, Amendment 10 for 32PTH1 DSC in HSM-H as documented in the corresponding SER [2] in Section 4.6.3.2. The results of the confirmatory analysis show that:

> "...the modeling approach used in the SAR is conservative, in that it tends to over-estimate the DSC shell temperatures, and predicts a greater area of the DSC surface to be at the higher temperatures. The component temperatures reported in the SAR for the HSM-H have a similar conservative bias"
>
> and
>
> "...the temperature results obtained with the StarCD model tend to confirm that the ANSYS model used in the thermal analysis of the HSM-H is conservative. The comparison for the most limiting case (DSC with Type 1 basket, HLZC #1, 40.8 kW) indicates that the HSM-H peak temperatures and the DSC shell temperatures are conservative with respect to a CFD model that represents the HSM-H and DSC as an integrated system."

Based on the results of the confirmatory analysis presented in Table 4.22 of the SER [2], the peak DSC shell temperature predicted by the ANSYS model is 50 °F higher compared to the StarCD model as shown in Table 4.22 [2]. Further, as shown in Table 4.23 of the SER [2], when using the conservative DSC shell temperature profile from the ANSYS model, the maximum fuel cladding temperature is higher by 40 °F when compared to the StarCD model.

This shows that the ANSYS model developed for evaluation of the HSM-H over predicts the maximum fuel cladding temperatures and DSC shell temperatures by a large extent. Similar temperature difference is expected for the AHSM-HS loaded with the 32PTH2 DSC model used in the UFSAR since AHSM-H storage module and the 32PTH2 DSC shell described in this application are almost identical to the HSM-H storage module and 32PTH1 DSC shell evaluated in the SER [2].

Since the methodology to evaluate the HSM-H or AHSM-HS, including the DSC shell, temperature profile has been reviewed and validated multiple times by the NRC in previous applications and found to be conservative, the uncertainty in the DSC temperature distribution was not included in the determination of the discretization error in the current UFSAR. The model for the DSC and its contents is the only new component, which could include uncertainties. Therefore, the determination of the discretization error addressed in previous RAI 4-14 was focused on the DSC model in the UFSAR.

No UFSAR changes were made.

**References**

1. Transnuclear Inc., Updated Final Safety Analysis Report for the Standardized NUHOMS® Horizontal Modular Storage System for Irradiated Nuclear Fuel, NUH-003, Revision 12, USNRC Docket No. 72-1004.
2. USNRC, "Final Safety Evaluation Report Transnuclear, Inc. Standardized NUHOMS® Horizontal Modular Storage System for Irradiated Nuclear Fuel," Docket No. 72-1004 Amendment No. 10 (ADAMS Accession No. ML092290329).
3. Transnuclear Inc., NUHOMS® HD, Horizontal Modular Storage System for Irradiated Nuclear Fuel, Updated Final Safety Analysis Report, Revision 3, USNRC Docket No. 72-1030.
4. U.S. Nuclear Regulatory Commission, "Safety Evaluation Report for the Transnuclear Inc., NUHOMS® HD Horizontal Modular Storage System for Irradiated Nuclear Fuel, Docket No. 72-1030," January 10, 2007 (ADAMS Accession No. ML070160089).

4-2 Demonstrate that the results from the grids used in the grid convergence studies can be represented as a normal distribution in order to obtain the discretization error. Otherwise, use the GCI to obtain the discretization error.

Table B.4.6-22 of FSAR Revision 3 provides the calculated discretization error. However, the error is calculated assuming the results from the grid study follow a Gaussian (normal) distribution. For additional information, see page 14 of ASME V&V 20-2009.

This information is needed to determine compliance with 10 CFR 72.236.

**RESPONSE TO RAI 4-2**

The results of the grid convergence studies presented in UFSAR Section B.4.6 are revised to use the GCI in determining the discretization error, as suggested.

4-3 Replace the ANSYS analysis of the transfer cask case which includes air circulation with the CFD analysis performed to provide the response to RAI 4-7.

In Calculation No. 13206-0416 the applicant concluded that the ANSYS approach (including the Flow Rate Model described in the FSAR) predicts slightly lower temperatures. The staff does not consider the temperature difference a slight change (18°F in addition to the modeling and discretization error). As predicted by the CFD analysis, the ANSYS predicted peak cladding temperatures are not conservative.

This information is needed to determine compliance with 10 CFR 72.236.

**RESPONSE TO RAI 4-3**

The UFSAR is revised to include the CFD analysis for the transfer cask case with air circulation. The CFD analysis of the OS200FC TC with the DSC, basket and fuel assemblies is identified as the design basis thermal evaluation that shall be used for any future evaluation for that condition.

In addition to the CFD analysis, the ANSYS air circulation model had to be retained as it provides the initial conditions for Load Case T10 and provides the DSC shell temperatures as criteria to reach steady-state conditions in continuation of Load Case T7.

However, UFSAR Sections B.4.1, B.4.5, B.4.6, and B.4.10 are revised to justify the limited applicability of the ANSYS air circulation model and to note that the ANSYS air circulation model shall not be used in the future for any other thermal evaluation of the OS200FC TC.

4-4 Obtain the analysis discretization error for the CFD analysis described in response to RAI 4-7 using the entire modeled geometry and not just a slice of the model by calculating the GCI following the procedure described in American Society of Mechanical Engineers Verification and Validation 20-2009 (ASME V&V 20-2009), "Standard for Verification and Validation in Computational Fluid Dynamics and Heat Transfer".

The CFD model used to obtain the GCI appears to represent only a slice of the model and not the entire geometry. As such, this model does not appear to capture the heat transfer and fluid flow characteristics of the intended geometry which includes specified mass flow rate at the inlet and a pressure boundary at the outlet (see response to RAI 4-14).

This information is needed to determine compliance with 10 CFR 72.236.

**RESPONSE TO RAI 4-4**

The CFD model used to obtain the GCI uses the entire modeled geometry. Only slices of the entire CFD model were selected to visualize the mesh density in the depictions shown in Figure A-2 of Calculation 13206-0416, Rev. 0 (provided as Enclosure 3 to TN-E-34062 on December 11, 2012). Since the mesh density of some of the models used for the GCI studies is too dense, showing the entire model in those depictions would have resulted in illegible pictures. The computation files submitted in Enclosure 5 to TN E-34062 in response to RAI 4-7 provide the evidence that the entire geometry was used for the GCI study of the CFD model. Clarifications are added in the description of the GCI study for the CFD model in UFSAR Section B.4.5.4.3.1 to avoid the appearance of using a slice model from the GCI study.

List of Changed and New UFSAR Pages, with Associated RAIs

| Changed Page | Reason for change |
|---|---|
| B.4.1-2 | RAI 4-3 |
| B.4.5-4 | RAI 4-3 |
| B.4.5-5 | RAI 4-3 |
| B.4.5-6 | RAI 4-3 |
| B.4.5-7 | RAI 4-3 |
| B.4.5-8 | text shift |
| B.4.5-9 | RAI 4-3 |
| B.4.5-9a | RAI 4-3 |
| B.4.5-12 | RAI 4-3 |
| B.4.5-13 | RAI 4-3 |
| B.4.5-13a | RAI 4-3, RAI 4-4 |
| B.4.5-13b | RAI 4-3 |
| B.4.5-13c | RAI 4-3, deleted |
| B.4.5-13d | RAI 4-3, deleted |
| B.4.5-13e | RAI 4-3, deleted |
| B.4.5-13f | RAI 4-3, deleted |
| B.4.5-13g | RAI 4-3, deleted |
| B.4.5-13h | RAI 4-3, deleted |
| B.4.5-15 | RAI 4-3 |
| B.4.5-16 | RAI 4-3 |
| B.4.5-19 | RAI 4-3 |
| B.4.5-20 | RAI 4-3 |
| B.4.5-21a | RAI 4-3 |
| B.4.5-21b | RAI 4-3 |
| B.4.5-21c | RAI 4-3 |
| B.4.5-21d | RAI 4-3, deleted |
| B.4.5-21e | RAI 4-3, deleted |
| B.4.5-21f | RAI 4-3, deleted |
| B.4.5-21g | RAI 4-3, deleted |
| B.4.5-22 | RAI 4-3 |
| B.4.5-24 | RAI 4-3 |
| B.4.5-28 | RAI 4-3 |
| B.4.5-31a | RAI 4-3 |
| B.4.5-31b | RAI 4-3 |
| B.4.5-31c | RAI 4-3 |
| B.4.5-31d | RAI 4-3 |
| B.4.5-31e | RAI 4-3 |
| B.4.5-31f | RAI 4-3, deleted |
| B.4.5-31g | RAI 4-3, deleted |

| Changed Page | Reason for change |
|---|---|
| B.4.5-31h | RAI 4-3, deleted |
| B.4.5-31i | RAI 4-3, deleted |
| B.4.5-31j | RAI 4-3, deleted |
| B.4.6-1 | RAI 4-3 |
| B.4.6-1a | text shift – new page |
| B.4.6-14c | RAI 4-2 |
| B.4.6-14d | RAI 4-2 |
| B.4.6-14e | RAI 4-2 |
| B.4.6-16 | RAI 4-3 |
| B.4.6-17 | text shift |
| B.4.6-31 | RAI 4-3 |
| B.4.6-33 | RAI 4-3 |
| B.4.6-34 | RAI 4-3 |
| B.4.6-35b | RAI 4-2 |
| B.4.6-49 | RAI 4-3 |
| B.4.6-55 | RAI 4-2 |
| B.4.10-2 | RAI 4-3 |
| B.4.10-3 | RAI 4-3 |

## Enclosure 3 to TN E-35275

# Changed and New UFSAR Pages

allowable temperatures are presented and comparisons are made with calculated temperatures as the basis for acceptance.

A total of four heat load zoning configurations (HLZCs) are allowed for the 32PTH2 DSCs as shown in Chapter B.2, Figure B.2.1-1. The total heat loads per DSC are 37.2 kW for HLZC # 1, 35.0 kW for HLZC # 2, 32.0 kW for HLZC # 3, and 31.2 kW for HLZC # 4.

ANSYS computer code, Version 10.0 [B4.26] is used for the thermal analyses of NUHOMS® 32PTH2 system. ANSYS is a comprehensive thermal, structural and fluid flow analysis package. It is a finite element analysis code capable of solving steady state and transient thermal analysis problems in one, two or three dimensions. Heat transfer via a combination of conduction, radiation and convection can be modeled by ANSYS.

The storage module AHSM-HS is used to store the 32PTH2 DSC. This module is thermally identical to the HSM-H module described in Appendix U, Section U.1.2.1.2 of the UFSAR for the Standardized NUHOMS® System [B4.22]. The thermal performance of the HSM-H was evaluated for a maximum decay heat load of 40.8 kW for 24PTH DSC and 32PTH1 DSC and a maximum heat load of 31.2 kW for 61BTH DSC as documented in Appendix P, Section P.4.4, Appendix T, Section T.4.4, and Appendix U, Section U.4.4, respectively, of the UFSAR for the Standardized NUHOMS® System [B4.22]. The same methodologies used for the thermal evaluation of the HSM-H in Appendix U, Section U.4.4 of the Standardized NUHOMS® System UFSAR [B4.22] are used in this chapter to evaluate the thermal performance of the AHSM-HS with the 32PTH2 DSC.

The thermal performance of the OS200FC Transfer Cask (TC) was previously evaluated for the 32PTH1 DSC with a maximum heat load of 40.8 kW as documented in Appendix U, Section U.4.5 of the UFSAR for the Standardized NUHOMS® System [B4.22]. The methodology used in Appendix U, Section U.4.5 of the Standardized NUHOMS® System UFSAR provides the basis for the thermal evaluation of the OS200FC TC with the 32PTH2 DSC in this chapter. It should be noted that computer codes Thermal Desktop and SINDA/FLUINT were used in Appendix U, Section U.4.5 of the Standardized NUHOMS® System UFSAR for the thermal evaluation of the OS200FC TC. However, ANSYS computer code is used in this chapter for the analysis of the OS200FC TC. *In the case that air circulation through the TC/DSC annulus is used as a recovery option, the thermal evaluation of the OS200FC TC is performed via a CFD model using ANSYS FLUENT computer code, Version 14.0 [B4.23].*

Analyses results for the AHSM-HS are provided in Section B.4.4, for the OS200FC TC in Section B.4.5, for the 32PTH2 DSC in Section B.4.6, and for loading/unloading conditions in Section B.4.8. A summary of the results from the analyses performed for normal, off-normal, and accident conditions, as well as maximum and minimum allowable temperatures, is provided in Table B.4.1-1, Table B.4.1-2, and Table B.4.1-3, respectively. The thermal evaluation concludes that with these heat loads, all design criteria for the NUHOMS® 32PTH2 system are satisfied for normal, off-normal, and accident conditions.

Load Case T10 is applicable to two conditions. The first condition applies for an OS200FC TC with 32PTH2 DSC with a heat load greater than 31.2 kW. If the air circulation is activated as a recovery operation during transfer, the air circulation needs to be turned off before transferring the 32PTH2 DSC into the AHSM-HS storage module. This condition presents a routine transfer operation.

The second condition occurs in a postulated scenario wherein steady-state conditions are established with the air circulation in operation and, subsequently the air circulation is lost during transfer operation. To minimize the occurrence of this condition, the OS200FC TC skid is equipped with redundant industrial grade blowers and each one of these blowers is capable of supplying the required minimum airflow rate. These blowers are also powered with a redundant power supply.

Both the above scenarios i.e. turning off air circulation to offload the 32PTH2 DSC to AHSM-HS or failure of the air circulation will decrease the heat dissipation and will result in a gradual increase of the maximum temperatures of the OS200FC TC and 32PTH2 DSC components. Therefore, for these conditions, an additional time limit is calculated to complete the transfer of the 32PTH2 DSC from the OS200FC TC to the AHSM-HS or to restart the air circulation or initiate other recovery operations to ensure that the peak fuel cladding temperature remains below the temperature limit of 752 °F established in [B4.3].

As described above, Load Case T10 starts from a steady state condition with air circulation in operation. In order to estimate the duration needed for the 32PTH2 DSC to reach steady-state conditions, a transient thermal analysis is performed. For this analysis, the worst case hottest initial condition is considered, which corresponds to Load Case T7 at the end of the time limit for the transfer operation. The analysis applies the boundary conditions from Load Case T8 with air circulation in operation through the transient phase and considers the DSC shell temperature as criteria to reach the steady state condition.

For all the normal, off-normal hot conditions and accident design load cases considered in Table B.4.5-1, insolation is considered per 10 CFR 71.71 [B4.2].

### B.4.5.3 Thermal Analysis of OS200FC TC with 32PTH2 DSC

The purpose of the TC thermal analysis is to determine the maximum component temperatures including the 32PTH2 DSC shell temperatures, and to establish the time limits for completion of transfer operations during normal and off-normal conditions. *For all cases except for Load Case T8, t*he 32PTH2 DSC shell temperatures determined in the TC thermal analysis are then used as boundary conditions in a subsequent 32PTH2 DSC basket thermal analysis described in Section B.4.6 *to evaluate the maximum fuel cladding temperatures. For Load Case T8, the maximum fuel cladding temperature is determined within an integrated model of the TC, DSC, basket and fuel assemblies.*

The design of the OS200FC TC was described in [B4.22], Appendix U for transfer of the 32PTH1 DSC with a maximum heat load of 40.8 kW. The same TC is used for transfer of the 32PTH2 DSC without any modifications.

*Two* models are developed to analyze the thermal performance of the OS200FC TC with the 32PTH2 DSC.

- For the OS200FC TC without air circulation, which includes the accident conditions, a half-symmetric 3D *ANSYS finite element* model is used to analyze the thermal performance for steady-state and transient operations. This model is described in Section B.4.5.3.2.

- For the OS200FC TC with air circulation, a steady state thermal evaluation is performed using a half-symmetric 3D *ANSYS FLUENT CFD* model of the TC, *DSC, basket and fuel assemblies* to determine the maximum component temperatures. *This model is* described in Section B.4.5.3.1.

The OS200FC TC model with air circulation is used for Load Case T8 (Off-Normal Hot, Steady-State, Air Circulation) with the maximum heat load of 37.2 kW as listed in Table B.4.5-1.

*In addition to the CFD model, an ANSYS finite element model of the OS200FC TC is developed using the FLUID116 and LINK34 elements to imitate the CFD model in calculation of the DSC shell temperatures. For ease of reference, this model is assigned as ANSYS air circulation model in this evaluation. The ANSYS air circulation model is only used to provide initial conditions for Load Case T10 or to provide DSC shell temperatures as criteria to reach steady state conditions in continuation of Load Case T7. The ANSYS air circulation model is described in Section B.4.5.3.2.1. Based on discussion provided in Section B.4.5.4.3, the use of the ANSYS air circulation model is limited to the two cases described above and shall not be used for any other thermal evaluation of the OS200FC TC with air circulation.*

B.4.5.3.1 *Description of the ANSYS FLUENT CFD Model*

*The model for the OS200FC TC is created in SolidWorks CAD computer code based on the nominal dimensions of the TC, DSC and basket. The fuel assemblies are modeled as homogenized regions within the fuel compartments. The CAD model is then imported into ICEM meshing software.*

*The CFD model used to simulate the thermal response of the OS200FC TC represents a 180° segment of the cask. The use of a 180° model permits the accurate simulation of the temperature distribution within the cask when the cask is in the horizontal orientation and the axis of the DSC is eccentric to that of the cask. Figure B.4.5-11 presents a view of the CFD model of the cask with the DSC assembly and fuel assemblies.*

*The model uses 4,195,932 hexahedral elements and 4,329,789 nodes to define the complete CFD model. Figure B.4.5-12 presents a perspective view of the CFD model for the cask body and for the 32PTH2 DSC and basket with fuel assemblies.*

*An airflow rate of 450 cfm with a daily average temperature of 107 °F is considered for this evaluation, which results in a mass flow rate of 0.12085 kg/s for the half symmetric model. This mass flow rate is specified as the inlet boundary condition and pressure outlet boundary condition is specified at the cask lid slots. All surfaces are defined as walls except for interfaces and symmetry. The symmetry surface is defined as asymmetry boundary condition.*

*The maximum fuel assembly length in the 32PTH2 DSC is 176.8" with 150.0" active fuel length. The position of the active fuel in the 32PTH2 DSC model starts 4.0" from the bottom end of the 32PTH2 DSC cavity. The fuel assembly beyond the active fuel region is modeled as helium. This results in a reduction in the axial heat transfer within the 32PTH2 DSC and higher maximum fuel cladding temperature. No convection is considered within the DSC cavity.*

*The decay heat load is applied as heat generation over the elements representing homogenized fuel assemblies. The heat generation rate used in this analysis is calculated as follows.*

$$\dot{q}''' = \left( \frac{q}{a^2 L_a} \times PF \right) \times CF$$

*Where,*

$\dot{q}'''$ = *Decay heat load per FA, kW (Multiply by 3412.3 to convert to Btu/hr),*

$a$ = *Width of the fuel compartment = 8.65",*

$L_a$ =*Active fuel length = 150",*

$PF$ = *Peaking Factor (see Section B.4.6.4 for distribution of peaking factor),*

$CF$ = *correction factor = 1.025 assumed for 32PTH2 DSC*

*The base heat generation rate is multiplied by peaking factors along the axial fuel length to represent the axial decay heat profile. The correction factor of 1.016 computed in Section B.4.6.4 is increased to 1.025 to ensure that a heat load of 37.2 kW is generated within the fuel assemblies. The heat generation within the fuel assembles is implemented using a user defined function.*

*The insolance is applied as a heat flux over the TC outer surfaces using average insolance values from 10 CFR 71.71 [B4.2]. The insolation values are averaged over 24 hours and multiplied by the surface absorptivity factor to calculate the solar heat flux. The solar heat flux values used in the OS200FC TC model are summarized below.*

| Surface Material | Shape | Insolance over 12 hrs [B4.2] (gcal/cm$^2$) | Solar Absorptivity(1) | Total solar heat flux averaged over 24 hrs (Btu/hr-in$^2$) |
|---|---|---|---|---|
| Stainless Steel | Curved | 400 | 0.587 (2) | 0.250 |
| | Flat vertical | 200 | 0.587 (2) | 0.125 |

(1) See Section B.4.2(r) for surface properties.

(2) Solar absorptivity of stainless steel is taken equal to its emissivity.

*The TC outer surfaces were split into horizontal and vertical surfaces in order to define insolance separately. The horizontal surfaces were split into two halves, upper and lower. On the upper half insolance, convection and radiation boundary conditions are applied while on the*

*lower half only convection and radiation boundary conditions are applied. The net heat transfer due to convection, radiation and solar insolance on the outer surfaces of the TC is modeled using a user defined function. Figure B.4.5-13 shows the different surfaces used for insolance, convection, and radiation boundary conditions.*

*The basket plates were separated into horizontal and vertical basket plates within the meshing tool ICEM CFD. The effective conductivities of homogenized basket plates are calculated using an ANSYS model of the plates.*

*The Discrete Ordinates (DO) Radiation is used as the radiation model for this analysis since the DO model is capable of considering symmetric boundary conditions and computational cost is moderate for typical angular discretization, and memory requirements are modest.*

*Realizable k-ε model is used as the turbulence model for the current simulation. SIMPLEC scheme is used for pressure velocity coupling and second order discretization method is used to discretize the pressure. Second order upwind scheme is used to discretize the remaining parameters such as density, momentum, turbulent kinetic energy, turbulent dissipation rate, energy and discrete ordinates.*

*The ANSYS FLUENT CFD model of the OS200FC TC with air circulation is used only for evaluation of Load Case T8 as listed in Table B.4.5-1.*

B.4.5.3.2 OS200FC TC *ANSYS Finite Element* Model Description

The half-symmetric, three-dimensional finite element model of OS200FC TC loaded with 32PTH*2* DSC contains the cask shells, cask bottom plate, cask lid, DSC shell, and DSC end plates with a homogenized basket assembly. The OS200FC TC model with 32PTH2 DSC is shown in Figure B.4.5-2 and Figure B.4.5-3.

SOLID70 elements are used to model the components, including the gaseous gaps. SURF152 surface elements are used for applying the insolation boundary conditions. Radiation along the gap between the DSC and TC inner liner is modeled using the AUX12 processor with SHELL57 elements used to compute the form factors.

Decay heat load is applied as a uniform volumetric heat generated throughout the homogenized region of the basket assembly. The homogenized basket assembly is centered axially in the 32PTH2 DSC. A uniform gap of 0.75" is considered between the homogenized basket assembly and the top/bottom ends of the 32PTH2 DSC. This assumption reduces the axial heat transfer and maximizes the DSC shell temperature, which in turn results in higher fuel cladding temperature. The volumetric heat generation rate is calculated as:

$$q''' = \frac{Q}{\pi\,(D_i/2)^2\,L_b}$$

$q'''$ = Volumetric heat generation rate (Btu/hr-in$^3$)
Q = decay heat load (Btu/hr) (to convert from kW multiply by 3412.3)
$D_i$ = 32PTH2 DSC inner diameter (in)
$L_b$ = Length of basket assembly (in)

The applied decay heat values in the model are listed below.

| Heat Load (kW) | Heat Load (Btu/hr) | $D_i$ (in) | $L_b$ (in) | Volumetric Heat Generation (Btu/hr-in$^3$) |
|---|---|---|---|---|
| 37.2 | 126938 | 68.5 | 177.15 | 0.1944 |
| 32.0 | 109194 | | | 0.1673 |
| 31.2 | 106464 | | | 0.1631 |

The insolation is applied as a heat flux over the OS200FC TC outer surfaces using average insolation values from 10 CFR 71.71 [B4.2]. The insolation values are averaged over 24 hours and multiplied by the surface absorptivity factor to calculate the solar heat flux. The solar heat flux values used in the OS200FC TC model are summarized below.

| Surface Material | Shape | Insolance over 12 hrs [B4.2] (gcal/cm$^2$) | Solar Absorptivity(1) | Total solar heat flux averaged over 24 hrs (Btu/hr-in$^2$) |
|---|---|---|---|---|
| Stainless Steel | Curved | 400 | 0.587 (2) | 0.250 |
| | Flat vertical | 200 | 0.587 (2) | 0.125 |

(1) See Section B.4.2(r) for surface properties.
(2) Solar absorptivity of stainless steel is taken equal to its emissivity.

Convection and radiation heat transfer from the OS200FC TC outer surfaces are combined together as total heat transfer coefficients. The total heat transfer coefficients are calculated using free convection correlations from Rohsenow Handbook [B4.11] and are incorporated in the model using ANSYS macros.

The typical boundary conditions applied on the OS200FC TC model are shown in Figure B.4.5-4.

During transfer, when the OS200FC TC is in a horizontal orientation, the 32PTH2 DSC shell rests on two rails in the OS200FC TC. These rails are flat stainless steel plates welded to the inner shell of the TC. The thickness of the rail is 0.12". Considering an angle of 12° between the lower and vertical plane, the dimensions of the rail, the 32PTH2 DSC and inner OS200FC TC diameter, the centerline of the 32PTH2 DSC is shifted down within the OS200FC TC cavity by 0.26". The eccentric location of the 32PTH2 DSC within the TC cavity is accounted for in the model considering the above shift. The thermal resistance between the 32PTH2 DSC and the OS200FC TC rails is assumed to be approximately 2.7 Btu/hr-in$^2$-°F identical to that used in the TC model described in [B4.22], Appendix U, Section U.4.5.2.

During loading operations, the water level in the TC/DSC annulus is maintained 12" below the 32PTH2 DSC top and is open to atmospheric pressure until the 32PTH2 DSC is sealed. The

water level in the annulus will be *monitored* and replenished *as noted in Sections B.8.1.1.3 and B.8.1.1.4.* These operational requirements prevent annulus water from approaching boiling temperature and assure that the DSC shell temperature does not exceed the boiling temperature of water. Therefore, a conservative DSC shell temperature of 212 °F is used for establishing the initial conditions for the transient analyses in the OS200FC TC when the TC is in the vertical orientation and the TC/DSC annulus is filled with water (see Load Cases T11 and T12 listed in Table B.4.5-1) for initial conditions with 37.2 and 32.0 kW decay heat loads.

*For load cases where the TC is in the vertical orientation (Load Cases T5, T5A, T6, T11, and T12 described in Table B.4.5-1), in the ANSYS model, the top and bottom TC exterior surfaces are modeled as adiabatic surfaces with only the vertical exterior cylindrical surfaces dissipating heat to the ambient.*

Due to differences between the heat loads considered for 32PTH1 DSC and 32PTH2 DSC, the effective properties for the neutron shield segments are modified iteratively to accurately capture the temperature gradients across each of the 19 neutron shield segments in the axial direction. Calculation of the effective properties for the neutron shield segments is described in Section B.4.5.3.3.

*The OS200FC TC finite element ANSYS model is used for all load cases listed in Table B.4.5-1 except Load Case T8.*

B.4.5.3.2.1 OS200FC TC *ANSYS* Air Circulation *Model*

*In the ANSYS air circulation model, the a*ir circulation through the annulus of the TC/DSC is modeled using the FLUID116 and LINK34 elements. The FLUID116 elements model the air flow along the axial length of the TC/DSC annulus by conducting heat and transmitting the fluid between its nodes, whereas the LINK34 elements model the convection from the TC/DSC surfaces due to the air flow. The FLUID116 elements are modeled such that they are connected to the LINK34 convection elements.

Air circulation is conservatively omitted and air conduction only is assumed in the region between the TC support rails (i.e., approximately 150° to 180°) due to the narrowness of the gap between the 32PTH2 DSC and the TC inner liner.

Based on the mass flow rates obtained for each of the annular segments from 0° to 150° *using FLUID116 elements*, the convection heat transfer coefficients for the TC/DSC annulus are computed using the correlations for flow within ducts and pipes. The convection heat transfer coefficients are computed as a function of the local hydraulic diameter, the Reynolds number, and the thermophysical properties of air. These convection heat transfer coefficients are applied to the LINK34 elements using the mpdata,hf/mp,hf commands.

The correlations for the convection coefficients are identical to those used in the thermal analysis of the OS200FC TC with a 32PTH1 DSC in [B4.22], Appendix U, Section U.4.5 and are taken from equations 7, 43, 44, 45, 57, and 57a in Chapter 7 of [B4.12].

*The ANSYS air circulation model is only used to provide initial conditions for Load Case T10 or to provide DSC shell temperatures used as criteria to reach steady state conditions in continuation of Load Case T7. The ANSYS air circulation model is compared to the CFD model in Section B.4.5.4.3 to demonstrate its limited applicability for the above two cases. The use of the ANSYS air circulation model is limited to the two cases described above. Any other thermal evaluation of the OS200FC TC with air circulation shall be evaluated using the ANSYS FLUENT CFD model described in Section B.4.5.3.1.*

B.4.5.3.3 Effective Neutron Shield Properties

The neutron shield panel consists of a cylindrical shell welded to the TC structural shell and supported by 18 rings. Each of the 16 inner supporting rings has seven holes to allow filling and draining of water in or out of the panel. The water in the neutron shield panel is modeled as 17 individual, cylindrical segments using SOLID70 elements as shown in Figure B.4.5-2.

For practical purposes, the time limits for vertical or horizontal transfer operations should be considered after sealing the 32PTH2 DSC when the water in the TC/DSC annulus starts to drain.

Based on the transient thermal analyses a maximum duration of 36 hours is allowed for both the normal, hot, vertical loading operations (Load Case T6) and the off-normal, hot, horizontal transfer operations (Load Case T7). Table B.4.5-5 summarizes the maximum temperatures for the OS200FC TC components and shows that the maximum TC component temperatures are below the allowable limits for duration of 36 hours for these two load cases.

Figure B.4.5-6 shows the temperature distribution of the OS200FC TC and 32PTH2 DSC for transient, off-normal, hot, horizontal transfer conditions (Load Case T7) at 36 hours.

B.4.5.4.3 Normal / Off-Normal Transfer Conditions with Air Circulation for Heat Loads > 32.0 kW and ≤ 37.2 kW

Steady state thermal analysis is performed for the OS200FC TC with 32PTH2 DSC and 37.2 kW heat load with air circulation for off-normal, hot, horizontal transfer conditions (Load Case T8) *using an ANSYS FLUENT CFD model* to demonstrate that the maximum TC component temperatures remain below the allowable limits once the air circulation is activated. Table B.4.5-6 summarizes the maximum temperatures for this load case. The temperature profiles for Load Case T8 are presented in Figure B.4.5-7. The peak fuel cladding and basket assembly component temperatures *are directly determined in the CFD model used for evaluation of Load Case T8. These values are reported* in Section B.4.6. *To determine the discretization error of the CFD model, a grid convergence study is performed as described in Section B.4.5.4.3.1. This study shows that the calculated maximum cladding temperature, including the discretization error, remain well below the allowable limits.*

A transient thermal analysis is performed for the OS200FC TC with 32PTH2 DSC and 37.2 kW heat load without air circulation to analyze the thermal performance of the system if the air circulation is turned off or lost (Load Case T10) to determine the DSC shell temperature profile and the maximum TC component temperatures. This analysis assumes that the transient begins with TC and DSC at steady-state conditions from Load Case T8. At time = 0, the fan airflow is turned off or lost and the system starts to heat up. Based on the transient thermal analysis a maximum duration of 12 hours is available to complete the transfer of the DSC to the AHSM-HS or to re-establish the air circulation.

*The initial temperatures for the DSC shell and TC components for this load case are determined using the ANSYS air circulation model described in Section B.4.5.3.2.1. To demonstrate that using these temperatures as initial conditions is valid, the results from the ANSYS FLUENT CFD model are compared with the results from the ANSYS air circulation model performed for Load Case T8 in Table B.4.5-12. As seen in Table B.4.5-12, the maximum DSC shell temperature predicted by the CFD model is only 2 °F higher than the value predicted by the ANSYS air circulation model. The maximum TC component temperatures predicted by the CFD model are at most 8 °F higher than the values predicted by the ANSYS air circulation model. Since the heat capacity of the system remains the same, the temperature increase or heat up rate observed once the air circulation is turned off would be the same with the only difference being the temperature*

*difference at the initial conditions. To conservatively bound the effect of the lower initial conditions, the maximum temperature differences described above are added to the respective component temperatures. The resulting temperatures are shown in Table B.4.5-7. The fact that the values resulting from the ANSYS air circulation model are used only as initial condition for Load Case T10, and Load Case T10 does not use air circulation to determine the time limit to complete the transfer of the DSC to the AHSM-HS, the maximum duration of 12 hours determined using this approach to maintain the maximum fuel cladding temperature below the allowable limit of 752 °F is reasonable. As noted in Section B.4.5.3.2.1, due to the uncertainties involved in the ANSYS air circulation model, any future thermal evaluation of the OS200FC TC with air circulation shall be performed using the ANSYS FLUENT CFD model described in Section B.4.5.3.1.*

Table B.4.5-7 summarizes the maximum temperatures for the OS200FC TC with 32PTH2 DSC and 37.2 kW heat load and shows that the maximum TC component temperatures are below the allowable limits.

As described in Section B.4.5.2, an additional transient analysis is performed to estimate the duration needed for the 32PTH2 DSC to reach the steady-state conditions when the air circulation starts at the end of the time limit for transfer operation. The initial condition for this analysis corresponds to Load Case T7 at 36 hours to bound the hottest expected temperatures during transfer operation before air circulation starts. The amount of time needed to use the air circulation is determined by comparison of the maximum DSC shell from this transient analysis to the maximum DSC shell temperature of 406 °F calculated for Load Case T8 (see Table B.4.5-6). Figure B.4.5-8 presents the maximum temperature history of the DSC shell once the air circulation is started at the end of Load Case T7. As seen from Figure B.4.5-8, the maximum DSC shell temperature decreases instantly once the air circulation is started and the maximum temperature decrease is observed within the first 6 hours after the start of air circulation. After 6 hours, the temperature decrease in the DSC shell temperature due to air circulation is approximately 1 °F/hr until 8 hours. The total temperature decrease of the DSC shell from 8 hours to 38 hours is approximately 3 °F (0.1 °F/hr). Due to small changes after 8 hours, it can be reasonably considered that using air circulation for 8 hours after achieving the time limit of 36 hours will decrease the DSC shell temperature from the hottest condition to the steady state level for the maximum heat load of 37.2 kW and maximum ambient temperature of 117 °F.

*The transient analysis described above is performed using the ANSYS air circulation model. As discussed for Load Case T10, the DSC shell temperature predicted by the ANSYS air circulation model is in good agreement with the DSC shell temperature predicted by the CFD model. Since the subject transient run uses the maximum DSC shell temperature to determine the duration required for the 32PTH2 DSC to reach the steady-state conditions include adequate accuracy. As noted previously, due to the uncertainties involved in ANSYS air circulation model, any future thermal evaluation of the OS200FC TC with air circulation shall be evaluated using the ANSYS FLUENT CFD model described in Section B.4.5.3.1.*

*B.4.5.4.3.1 Grid Convergence Study for the OS200FC TC CFD Model*

*The discretization error of the integrated CFD model representing the OS200FC TC, 32PTH2 DSC, basket, and fuel assemblies is performed using the methodology outlined in the ASME V&V 20-2009 [B4.33]. The steps used in this methodology are described in Section B.4.6.7.1.1.*

*Table B.4.5-9 shows the number of elements in the four different grid sizes considered for this evaluation along with the representative cell size (h) and the refinement factors (r). Table B.4.5-10 gives maximum fuel cladding temperatures for each level of grid. It can be observed that the maximum temperature is the same for all levels of grid refinement.*

*Table B.4.5-11 presents the results of the five steps specified in Section 5 of the ASME V&V 20-2009 [B4.33] and summarizes the grid convergence index of set # 1 and set # 2.*

*As seen from Table B.4.5-11, the order of accuracy (p) for Set # 1 is 13.84, which is much higher than the second order discretization scheme utilized in the FLUENT CFD described in Section B.4.5.3.1. This is because the Richardson extrapolation method does not work when $\varepsilon_{21} = \Phi_2 - \Phi_1$ or $\varepsilon_{32} = \Phi_3 - \Phi_2$ is close to zero as noted in [B4.36]. In the current evaluation, the temperature difference for Grid # 1 and Grid # 2 of Set # 1 is $\varepsilon_{32} = 0.03$ and is close to zero. Therefore, the GCI is not computed for this set.*

*However, the GCI is computed for Set # 2 with a fourth grid which is further refined. As seen from Table B.4.5-11, for this set the GCI is 9.86 °F. Based on the information regarding GCI from [B4.35],*

> *"...the GCI is a measure of the percentage the computed value is away from the value of the asymptotic numerical value. It indicates an error band on how far the solution is from the asymptotic value. It indicates how much the solution would change with a further refinement of the grid. A small value of GCI indicates that the computation is within the asymptotic range..."*

*Therefore, this small value of GCI indicates that the computed maximum fuel cladding is close to the asymptotic value and therefore the computed results are within the asymptotic range.*

*Further, as seen from Table B.4.5-11, an observed order of accuracy (p) for Set # 2 is calculated to be 0.6, which is lower than the theoretical order of accuracy. This might be due to the slight difference in the refinement factors and due to the small differences in the temperature with increasing grid refinement. Additional refinement of the grids might successfully improve the order of accuracy, however the finest grid currently used has slightly greater than 9 million elements and refining further with a minimum refinement factor (h) of 1.3 will cause the next grid to have at least 22 million elements. This level of refinement is computationally prohibitive and is not needed since the maximum temperatures decrease with increasing refinement.*

*Figure B.4.5-14 shows the maximum fuel cladding temperature as a function of the number of elements. As seen from the Figure B.4.5-14, the maximum fuel cladding temperatures resulting from the various grids display monotonic convergence. As it can be observed, the change in the maximum temperature is insignificant with the increase in refinement of the grid. Figure B.4.5-15 shows the grid density of the models used for the grid convergence study. To illustrate the grid density only a slice of the CFD model is selected for these depictions.*

B.4.5.4.4 Accident Conditions

As noted in Section B.4.5.2, the loss of neutron shield and loss of air circulation is bounding for the fire accident case. The maximum temperatures for the bounding loss of neutron shield and loss of air circulation steady-state accident condition (Load Case T9) are presented in Table B.4.5-8. As seen from Table B.4.5-8, maximum component temperatures are below the allowable limits. Figure B.4.5-9 presents the temperature profiles for the loss of neutron shield and loss of air circulation accident condition for the OS200FC TC with 32PTH2 DSC and 37.2 kW heat load.

B.4.5.5 Evaluation of OS200FC TC Performance

The thermal performance of the OS200FC TC is evaluated under normal, off-normal, and accident conditions of operation as described above and is shown to satisfy all the temperature limits and criteria. The DSC shell temperatures calculated here are used in the DSC basket and fuel cladding models as a boundary condition in Section B.4.6. The results show that all the basket and fuel cladding material temperature limits are also satisfied.

Based on the discussions presented in Sections B.4.5.2 and B.4.5.4, time limits for transfer operations are necessary to maintain the fuel cladding temperature and the OS200FC TC components temperatures below the allowable limits. Figure B.4.5-10 presents an overview of the transfer operations for OS200FC TC with 32PTH2 DSC.

**Table B.4.5-2**
***Not Used***

**Table B.4.5-3**
***Not Used***

**Table B.4.5-6**
**Maximum Temperatures of OS200FC TC with 32PTH2 DSC @ 37.2 kW, With Air Circulation**

| | Off-Normal Hot, Horizontal, Steady-State with Air Circulation Load Case T8 | Max. Allowable (°F) |
|---|---|---|
| **Time** | No time limit | |
| **Component** | $T_{max}$ (°F) | |
| DSC *Cylindrical* Shell | *408* | --- |
| Inner Liner | *338* | --- |
| Gamma Shield | *331* | 620 [B4.13] |
| Structural Shell | *279* | --- |
| Neutron Shield, Max. / Avg. | *274 / < 274* | -- / 290 (2) |
| Neutron Shield Outer Skin | *263* | --- |
| Air, Inlet / Exit | *107 / 259* | --- |
| Bulk Average NS-3 | *211* | 250 / 300 (1) |
| Closure Lid | *252* | --- |
| Top Forging | *263* | --- |
| Bottom Forging | *166* | --- |

(1) For NS-3, 250 °F is the temperature limit for long-term operations and 300 °F is the temperature limit for short-term normal operations like vertical loading.

(2) Bulk average temperature of water in the neutron shield is limited by the 45 psig pressure relief valves on the shield. The equivalent steam saturation temperature at this pressure is approximately 290 °F.

**Table B.4.5-7**
**Maximum Temperatures of OS200FC TC with 32PTH2 DSC @ 37.2 kW,**
**Air Circulation Turned Off / Air Circulation Failure during Transfer Operations**

| | Air Circulation turned-off or Air Circulation failure during transfer operation Load Case T10 | Max. Allowable (°F) |
|---|---|---|
| **Time** | 12 hrs | |
| **Component** | **$T_{max}$ (°F)** | |
| DSC *Cylindrical* Shell | *446* | --- |
| Inner Liner | *339* | --- |
| Gamma Shield | *333* | 620 [B4.13] |
| Structural Shell | *281* | --- |
| Neutron Shield, Max. / Avg. | *276 / 239* | -- / 290 (2) |
| Neutron Shield Outer Skin | *265* | --- |
| Bulk Average NS-3 | *193* | 250 / 300 (1) |
| Closure Lid | *242* | --- |
| Top Forging | 287 | --- |
| Bottom Forging | 220 | --- |

(1) For NS-3, 250 °F is the temperature limit for long-term operations and 300 °F is the temperature limit for short-term normal operations like vertical loading.

(2) Bulk average temperature of water in the neutron shield is limited by the 45 psig pressure relief valves on the shield. The equivalent steam saturation temperature at this pressure is approximately 290 °F.

***Table B.4.5-9***
***Grid Sizes and Refinement Factors for CFD model***

| | Set # 1 (Grid # 1,2,3) | Set # 2 (Grid # 2,3,4) |
|---|---|---|
| $N_1$ | 4196112 (Grid # 3) | 9218858 (Grid #4) |
| $N_2$ | 1925705 (Grid # 2) | 4196112 (Grid #3) |
| $N_3$ | 876515 (Grid # 1) | 1925705 (Grid #2) |
| $h_1$ | 0.45 | 0.34 |
| $h_2$ | 0.58 | 0.45 |
| $h_3$ | 0.76 | 0.58 |
| $r_{21}$ | 1.296 | 1.299 |
| $r_{32}$ | 1.3 | 1.296 |

***Table B.4.5-10***
***Maximum Fuel Cladding Temperatures***

| | Set # 1 (Grid # 1,2,3) | Set # 2 (Grid # 2,3,4) |
|---|---|---|
| $\Phi_1$ (°F) | 710.660 | 709.285 |
| $\Phi_2$ (°F) | 711.764 | 710.660 |
| $\Phi_3$ (°F) | 711.798 | 711.764 |
| $\Phi_{Avg}$ (oF) | 711.407 | 710.67 |
| $\varepsilon_{21} = \Phi_2 - \Phi_1$ (°F) | 1.10 | 1.38 |
| $\varepsilon_{31} = \Phi_3 - \Phi_2$ (°F) | 0.03 | 1.10 |

*Table B.4.5-11*
*Discretization Error of the CFD Model*

| | Uncertainty in Maximum Fuel Cladding | |
|---|---|---|
| | Set # 1 | Set # 2 |
| | Grid # 1, 2,3 | Grid # 2,3,4 |
| $N_1$ | 4196112 | 9218858 |
| $N_2$ | 1925705 | 4196112 |
| $N_3$ | 876515 | 1925705 |
| $h_1$ | 0.55 | 0.42 |
| $h_2$ | 0.71 | 0.55 |
| $h_3$ | 0.92 | 0.71 |
| $r_{21}$ | 1.29 | 1.31 |
| $r_{32}$ | 1.30 | 1.29 |
| $\Phi_1$ (°F) | 710.660 | 709.285 |
| $\Phi_2$ (°F) | 711.764 | 710.660 |
| $\Phi_3$ (°F) | 711.798 | 711.764 |
| $\Phi_{Avg}$ (°F) | 711.407 | 710.570 |
| $\varepsilon_{21} = \Phi_2 - \Phi_1$ | 1.10 | 1.38 |
| $\varepsilon_{32} = \Phi_3 - \Phi_2$ | 0.03 | 1.10 |
| $p$ | 13.84 | 0.60 |
| $\Phi^{21}_{ext}$ (°F) | -- | 701.40 |
| $e^{21}_{a}$ | -- | 1.38 |
| $F_s$ | -- | 1.25 |
| $GCI^{21}_{Fine}$ | -- | 9.86 |
| $U_{num}$ (°F) | -- | 9.86 |

*Table B.4.5-12*
*Component Temperature Comparison (Load Case # T8)*

| Time | ANSYS Air Circulation Model<br>No Time Limit | ANSYS FLUENT CFD Model<br>No Time Limit | | |
|---|---|---|---|---|
| **Component** | $T_{max}$ (°F) | $T_{max}$ (°F) | Difference (°F) | Max. Allowable (°F) |
| Fuel Cladding | 693 | 711 | 18 | 752 [B4.3] |
| Fuel Compartment | 668 | 685 | 17 | --- |
| Basket Rails | 467 | 490 | 23 | --- |
| DSC Cylindrical Shell | 406 | 408 | 2 | --- |
| Inner Liner | 330 | 338 | 8 | --- |
| Gamma Shield | 324 | 331 | 7 | 620 [B4.13] |
| Structural Shell | 273 | 279 | 6 | --- |
| Neutron Shield, Max. | 268 | 274 | 6 | 290 (2) |
| Neutron Shield Outer Skin | 257 | 263 | 6 | --- |
| Bulk Average NS-3 | 207 | 211 | 4 | 250 / 300 (1) |
| Closure Lid | 252 | 252 | 0 | --- |

(1) For NS-3, 250 °F is the temperature limit for long-term operations and 300 °F is the temperature limit for short-term normal operations like vertical loading.

(2) Bulk average temperature of water in the neutron shield is limited by the 45 psig pressure relief valves on the shield. The equivalent steam saturation temperature at this pressure is approximately 290 °F.

**Figure B.4.5-1**
***Not Used***

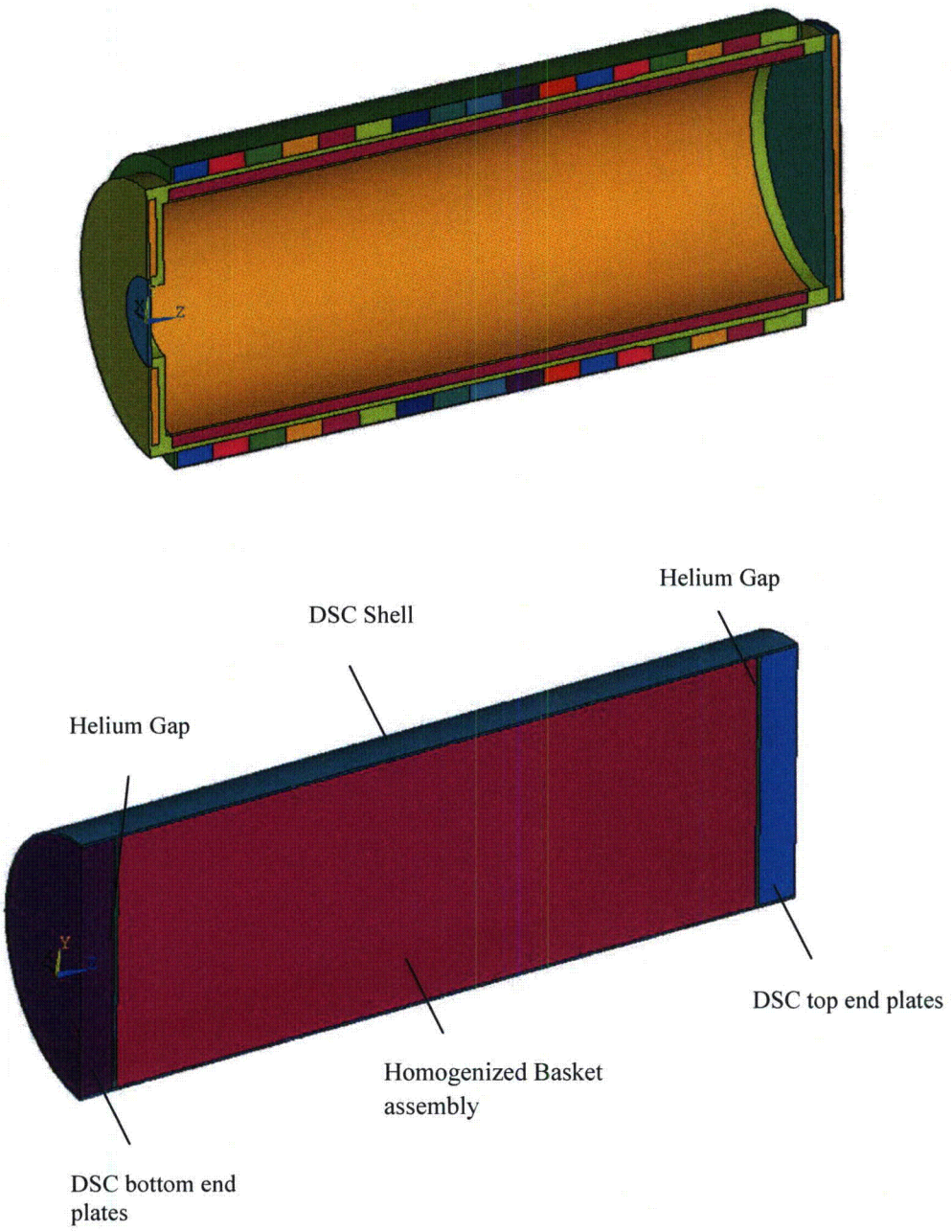


**Figure B.4.5-3**
**OS200FC TC Finite Element Model, Components**

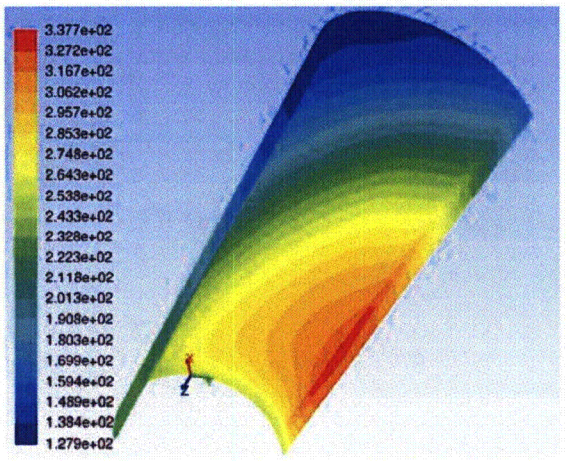


*Inner Liner*

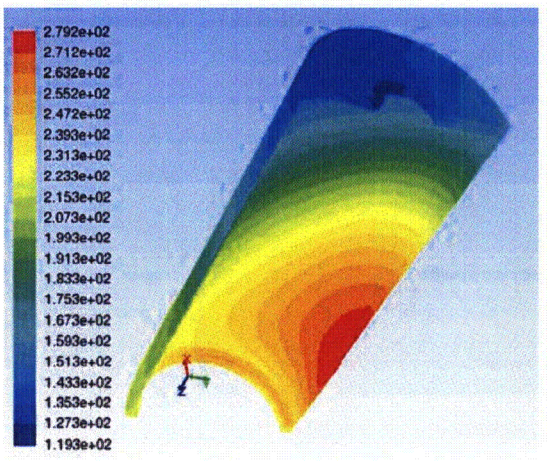


*Structural Shell*

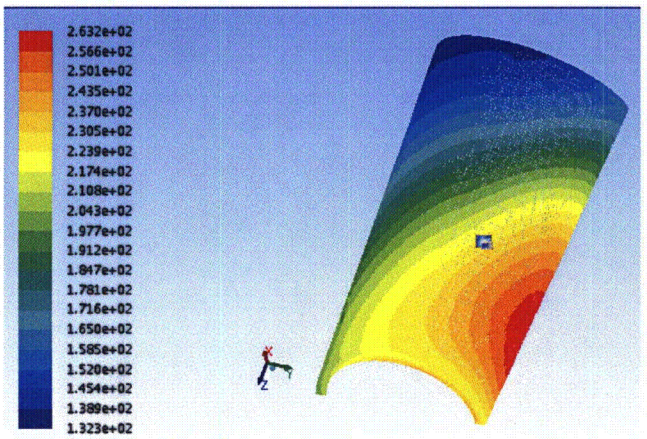


*Neutron Shield Outer Skin*

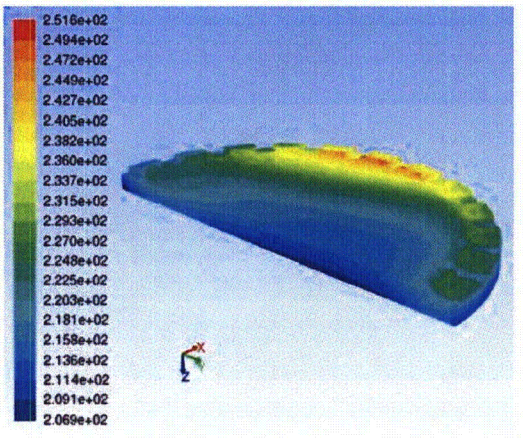


*Closure Lid (°F)*

**Figure B.4.5-7**
**Temperature Distribution for OS200FC TC with 32PTH2 DSC @ 37.2 kW, with Air Circulation, Off-Normal Hot, Horizontal Steady-State Operations (Load Case T8)**

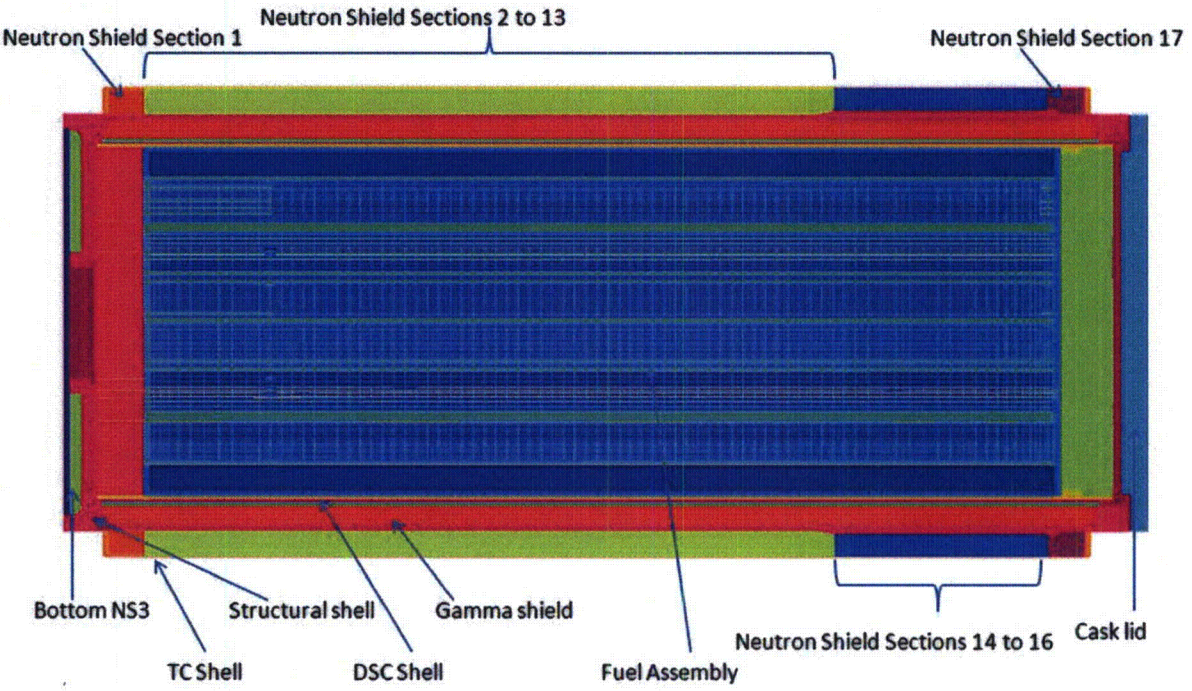


***Figure B.4.5-11***
***CFD Model of the OS200FC TC with the 32PTH2 DSC***

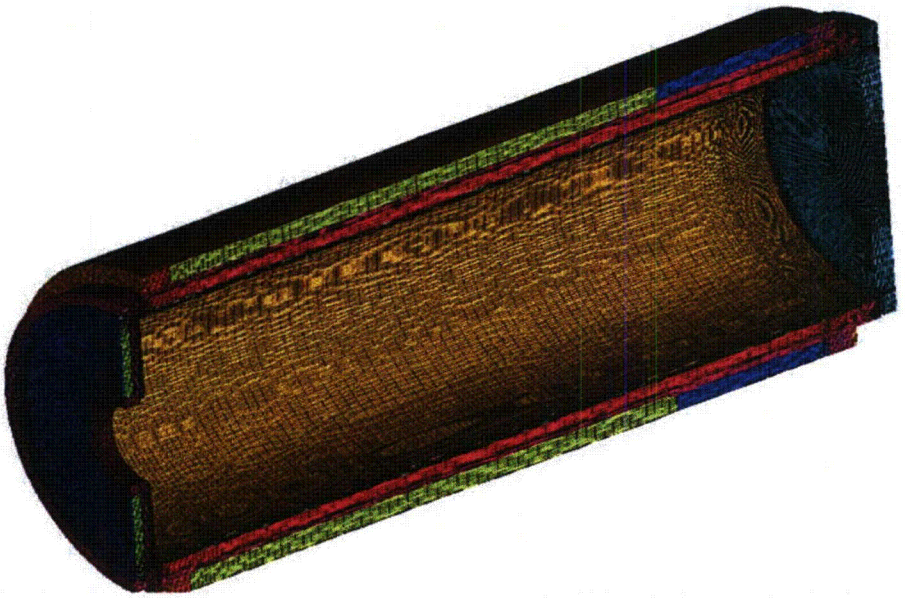

OS200FC TC

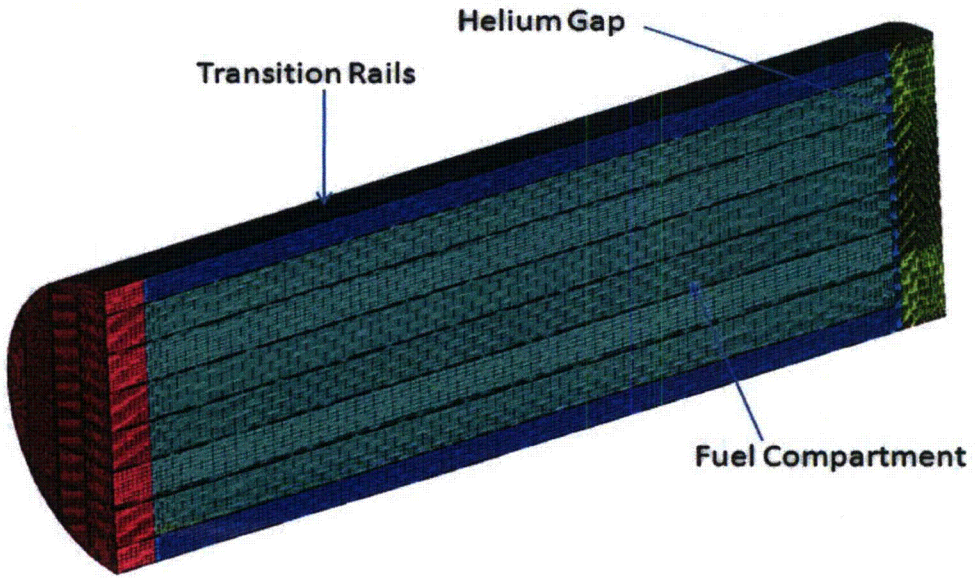


32PTH2 DSC

***Figure B.4.5-12***
***Detail of CFD Model of the OS200FC TC with the 32PTH2 DSC***

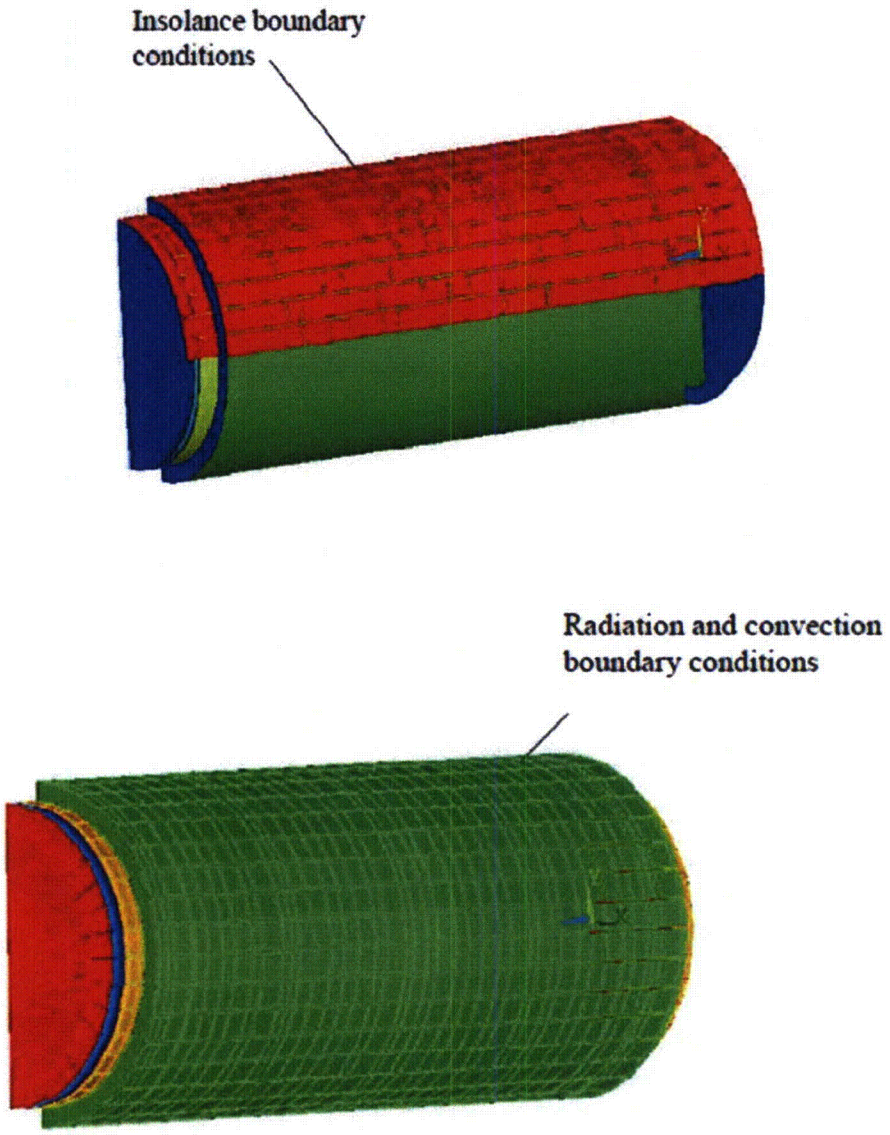


***Figure B.4.5-13***
***Boundary Conditions of the OS200FC TC CFD Model***

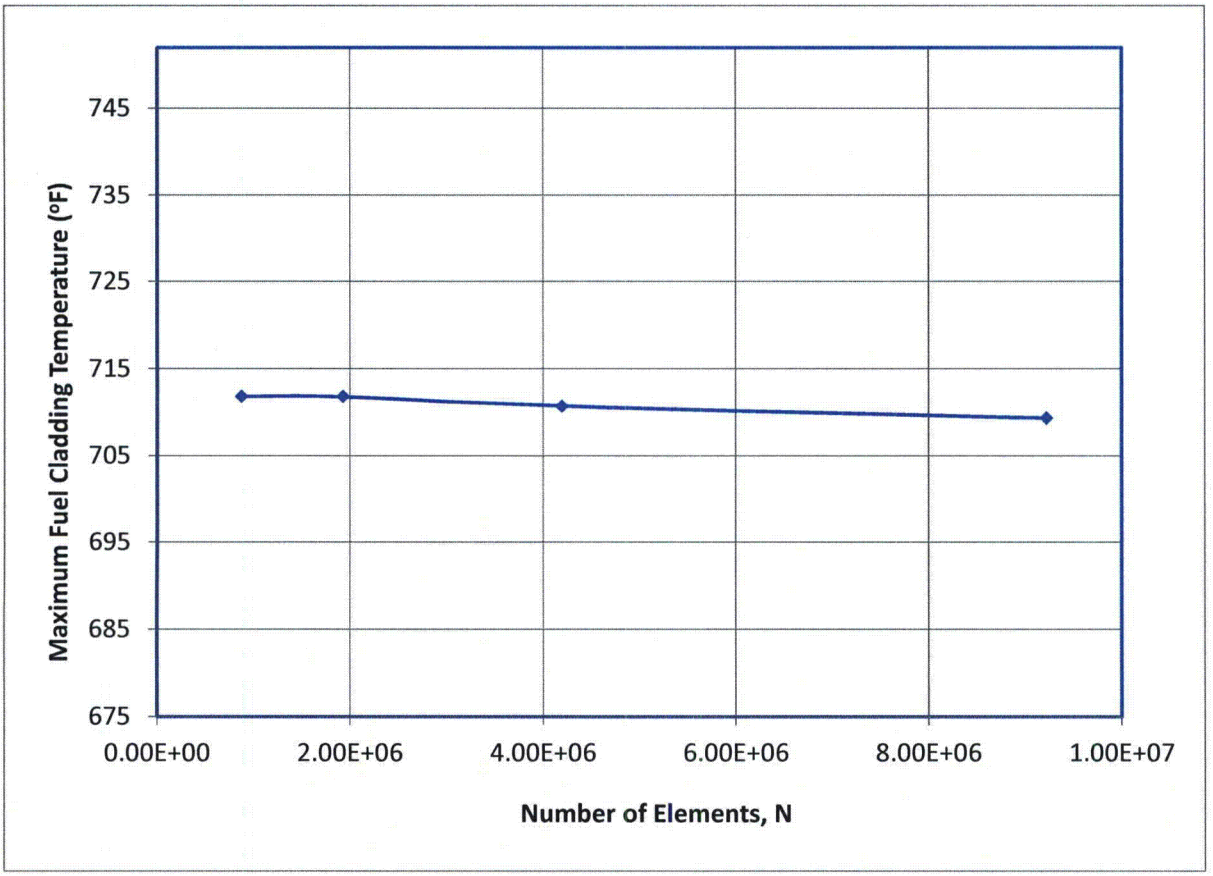


***Figure B.4.5-14***
***Maximum Fuel Cladding Temperature versus Number of Elements***

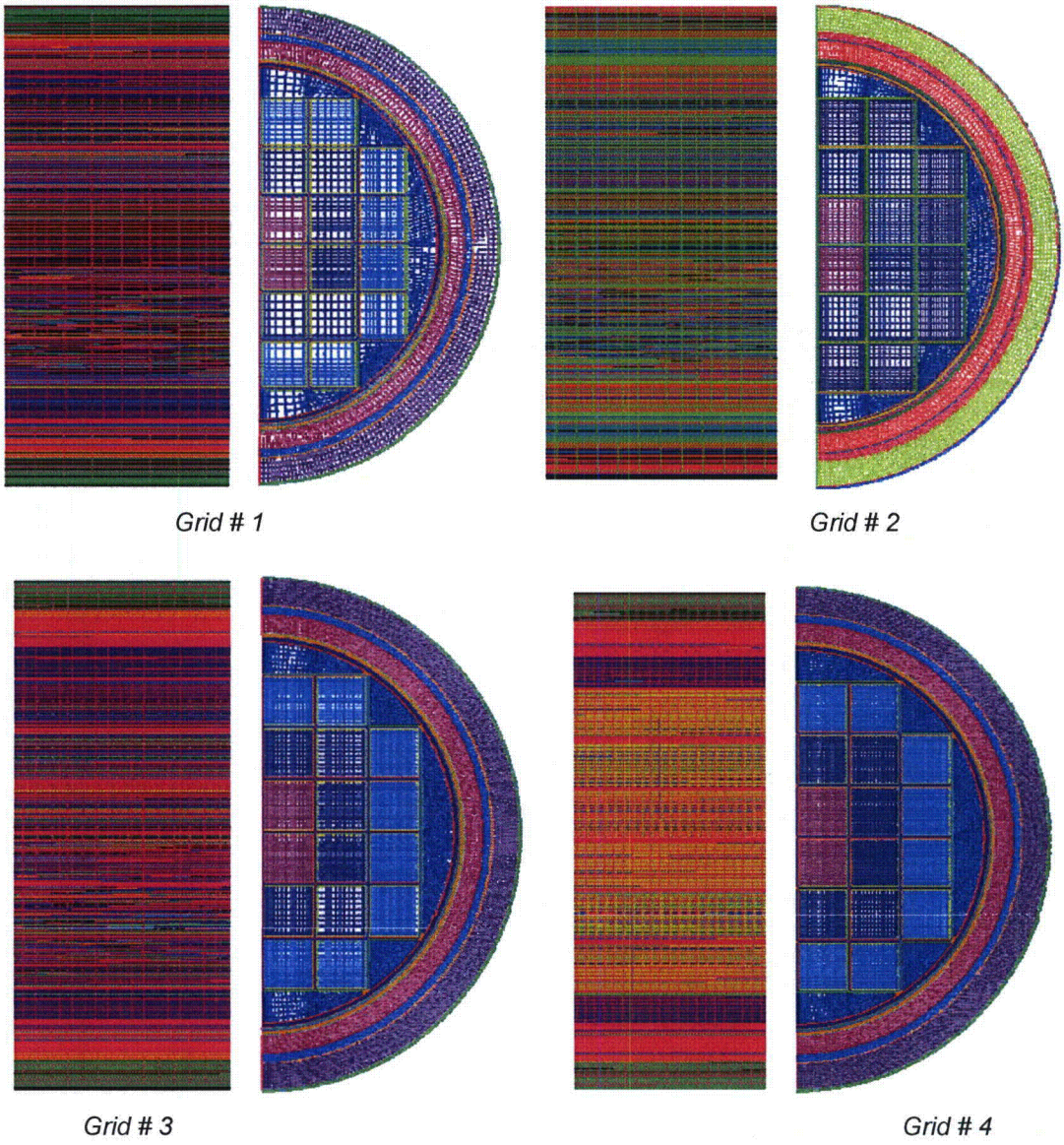


***Figure B.4.5-15***
***Model Grid Density Used for Grid Convergence Study***

## B.4.6 Thermal Evaluation of 32PTH2 DSC

The 32PTH2 DSC is designed to store 32 intact (or up to 16 damaged and remaining intact) fuel assemblies. Up to 16 damaged fuel assemblies (DFA) can be placed in cells located at the outer edge of the 32PTH2 basket assembly (Zone 3) as shown in Chapter B.2, Figures B.2.1-1.

The design of the 32PTH2 DSC is very similar to the 32PTH1 DSC described in [B4.22], Appendix U. The 32PTH1 DSC was evaluated based on a finite element model described in [B4.22], Appendix U, Section U.4.6. Due to similarities between the 32PTH1 and 32PTH2 DSCs, the 32PTH2 DSC is evaluated in this section using the same methodologies used to evaluate the 32PTH1 DSC in [B4.22].

*For Load Case T8 described in Section B.4.5, the maximum temperatures of the fuel cladding and basket components are determined using an integrated CFD model of the TC, DSC, basket and fuel assemblies. The CFD model for Load Case T8 is described in Section B.4.5.3.1. The results of the integrated CFD model for the fuel cladding and basket components are presented in this section.*

### B.4.6.1 Ambient Temperature Specification and Load Cases

The ambient temperatures for storage and transfer conditions are specified in Sections B.4.4.1 and B.4.5.1, respectively.

The load cases considered for evaluation of the NUHOMS® 32PTH2 system for storage and transfer conditions are described in Sections B.4.4.2 and B.4.5.2, respectively.

### B.4.6.2 Thermal Analysis of 32PTH2 DSC

The purpose of the 32PTH2 DSC thermal analysis is to determine the maximum temperatures of the fuel cladding and the basket components. As noted in Section B.4.4.3 and B.4.5.3, the DSC shell temperatures determined in the AHSM-HS and OS200FC TC thermal analyses are used as boundary conditions in the 32PTH2 DSC model to evaluate the maximum temperature under normal, off-normal, and accident conditions.

The thermal analysis of the NUHOMS® 32PTH2 DSC is based on a finite element model developed using the ANSYS computer code [B4.26]. The methodology used is identical to that used for the 32PTH1 DSC model described in Appendix U, Section U.4.6.

#### B.4.6.2.1 Description of the ANSYS Model of 32PTH2 DSC

A three-dimensional model representing the 32PTH2 DSC and basket is developed using ANSYS computer code [B4.26]. This model represents a longitudinally full-length, one-half (180°) cross section of the 32PTH2 DSC as shown in Figure B.4.6-1 through Figure B.4.6-4. The 32PTH2 DSC model comprises the shell assembly (including the shell, top/bottom cover plates, and shield plug plates), the basket assembly (including fuel compartments, aluminum and neutron absorber basket plates, and transition rails) and the homogenized fuel assemblies. All of these DSC components are modeled using SOLID70 elements. The following assumptions are considered for the 32PTH2 DSC model:

- The fuel assemblies contained in the DSC basket are intact fuel assemblies. Since the damaged fuel assemblies are loaded in the outermost fuel compartment cells, they do not affect the maximum temperatures or the maximum temperature gradients in this evaluation. A sensitivity analysis is conducted to capture the effects of the damaged fuel assemblies on

$$\phi_{ext}^{21} = (r_{21}^{p} * \phi_1 - \phi_2) / \left| r_{21}^{p} - 1 \right|$$

*The discretization error for the fine grid in each set is computed in Step 5 based on the relative error and the grid convergence index (GCI) between the fine and intermediate meshes in each set.*

*Step 5*

*The relative error based on equation 2-4-9 of ASME V&V 20-2009 [B4.33] is computed as:*

$$e_a^{21} = \left| \phi_1 - \phi_2 \right|$$

*Using the relative error, the GCI for the fine grid based on equation 2-4-12 of ASME V&V 20-2009 [B4.33] is computed as:*

$$GCI_{fine}^{21} = \frac{F_s * e_a^{21}}{r_{21}^{p} - 1}$$

*Since three grids are used, a factor of safety ($F_s$) equal to 1.25 is used as noted in Step 5, Section 2-4-1 of [B4.33]. The discretization error is considered equal to the GCI without any error distribution based on Page 14 of ASME V&V 20-2009 [B4.33]and is computed as:*

$$U_{num} = GCI_{fine}^{21}$$

*B.4.6.7.1.2 Computations for the Grid Convergence Study*

*As noted in Steps 1 and 2 of the methodology described in Section B.4.6.7.1.1, Load Case # S3 shown in Table B.4.6-14 is re-evaluated using the four grids listed in Table B.4.6-20 in two sets of calculations. As shown in Table B.4.6-20, the maximum number of elements for the 32PTH2 DSC model used in this study ranges from 223,080 elements to 2,981,768 elements. Out of the four grids considered, Grid # 3 with 1,267,792 is identical to the thermal model used for the thermal analysis in Section B.4.6.2. Therefore, the maximum fuel cladding temperature for Load Case # S3 as noted in Table B.4.6-14 is used in this study for Grid # 3.*

*For the remaining three grids, the ANSYS models are developed to determine the maximum fuel cladding temperature using the methodology described in Section B.4.6.2. Since the axial mesh density is altered for these grids, the peaking factors are updated based on the updated axial segments using the same methodology described in Section B.4.6.4. The peaking factors for Grid # 4 are not changed since it adds axial segments without altering the existing ones used in Section B.4.6.4.*

*Further, since the mesh is altered, the 32PTH2 DSC shell temperatures from the AHSM-HS in Section B.4.4.3 are mapped to the 32PTH2 DSC model.*

*The maximum fuel cladding temperatures resulting for each grid size are summarized in Table B.4.6-21. Using the maximum fuel cladding temperatures listed in Table B.4.6-21, the discretization error and the observed order of accuracy are computed using Steps 3 through 5 described in Section B.4.6.7.1.1.*

*B.4.6.7.1.3 Results and Discussion of the Grid Convergence Study*

*Using the methodology and the computations described in Sections B.4.6.7.1.1 and B.4.6.7.1.2, the grid convergence study is performed for the 32PTH2 DSC ANSYS finite element model. The results of the grid convergence study are listed in Table B.4.6-22.*

*As seen from Table B.4.6-22, the discretization error ($U_{num}$) is 6.24 °F for the fine grid in Set # 1 with Grids # 2, 3 and 4. Therefore, the maximum fuel cladding temperature for the fine grid within Set # 1 including the discretization error is 733.35 °F ($\Phi_1 + U_{num} = 727.11 + 6.24$).*

*Similarly as shown in Table B.4.6-22, the discretization error ($U_{num}$) is 2.70 °F for the fine grid in Set # 2 with Grids # 1, 2 and 3. Therefore, the maximum fuel cladding temperature for the fine grid within Set # 2 including the discretization error is 732.00 °F ($\Phi_1 + U_{num} = 729.30 + 2.70$).*

*The absolute discretization error for the fine grid in each set decreases with increase in the mesh refinement. Further, the maximum fuel cladding temperatures for both Set # 1 and Set # 2 including the discretization error, are approximately the same. This shows that the maximum fuel cladding temperatures determined using Grids # 3 and 4 are close to the asymptotic range of maximum fuel cladding temperatures with an absolute error of approximately 6 °F for Grid # 3.*

*In addition, based on the information regarding GCI from [B4.35],*

> *"...the GCI is a measure of the percentage the computed value is away from the value of the asymptotic numerical value. It indicates an error band on how far the solution is from the asymptotic value. It indicates how much the solution would change with a further refinement of the grid. A small value of GCI indicates that the computation is within the asymptotic range..."*

*The fine grid GCI is less than 1% for both sets, as shown in Table B.4.6-22. Based on the discussion in [B4.35], this small value of GCI indicates that the computed maximum fuel cladding is close to the asymptotic value and therefore the computed results are in the asymptotic range.*

*The observed order of accuracy (p) computed for both Set # 1 and Set # 2 is 2.17 and 2.39, respectively. The small difference in the observed order of accuracy (p) is due to the difference in the refinement factors between the two sets. The theoretical order of accuracy of the ANSYS solution is 2 as noted in Step 3 of Section B.4.6.7.1.1. This shows that the theoretical order of the ANSYS solution and the observed accuracy (p) are comparable.*

*Figure B.4.6-20, shows the maximum fuel cladding temperature as a function of the number of elements. As seen from Figure B.4.6-20, the maximum fuel cladding temperature resulting from the various grids display monotonic convergence. However, the amount of temperature increase*

*from one grid to the next is reduced with increase in the mesh refinement. Further, as seen from Table B.4.6-21 and Table B.4.6-22, an increase of 2.5 times in the element count from Grid # 3 with approximately 1.2 million elements to Grid # 4 with approximately 3 million elements results in a maximum fuel cladding temperature increase of 2 °F. This shows that the use of Grid # 3 to evaluate the thermal performance of the 32PTH2 DSC is acceptable.*

*Further, for all conditions of normal storage, the maximum fuel cladding is less than 727 °F as noted in Table B.4.6-14 with a margin of 25 °F to the fuel cladding temperature limit of 752 °F [B4.3]. This margin to the fuel cladding temperature is significantly larger than the maximum discretization error of 6 °F computed in Table B.4.6-22. Therefore, the thermal evaluation performed using Grid # 3 remains valid and acceptable.*

B.4.6.8 Sensitivity Study for Effects of Damaged Fuel Assemblies

The 32PTH2 DSC is designed to store 32 intact or up to 16 damaged and remaining intact fuel assemblies. Up to 16 damaged fuel assemblies can place in cells located at the outer edge of the 32PTH2 basket as shown in Chapter B.2, Figure B.2.1-1.

The cladding of damaged fuel assemblies can experience further damages due to a postulated drop accident considered during transfer operations in an OS200FC TC. To bound the effect of these damages, a sensitivity analysis is conducted considering the worst case condition, in which the damaged fuel assemblies become rubble. Following the rationale in NUREG/CR-6835 [B4.7], it is assumed that the fuel rods do not shatter into very small pieces and the fuel rubble is not in a tightly compacted mass. Instead, the fuel rubble is assumed to be 50% void by volume. To provide the maximum heat generation, the fuel rubble is assumed to be contained within the original active fuel volume, albeit in the lower portion of the original volume. Consistent with NUREG/CR-6835, the axial-burnup variation in the rubble is also assumed to be uniform. The heat generation rate used for the fuel rubble is calculated as:

temperatures for normal and off-normal storage conditions are assumed to occur for a sufficient duration such that a steady-state temperature distribution exists within the components.

*For Load Case T10, as stated in Section B.4.5.4.3, to conservatively bound the effect of the lower initial conditions, the maximum temperature difference for each component from Section 4.5, Table B.4.5-12 is added to the maximum temperatures calculated using the ANSYS finite element model.*

The maximum fuel cladding temperatures during normal, off-normal, and accident conditions of storage and transfer are listed in Table B.4.6-14 and Table B.4.6-15, respectively. The maximum temperatures of the basket assembly components are listed in Table B.4.6-16 and Table B.4.6-17 for storage and transfer conditions, respectively.

Figure B.4.6-9 and Figure B.4.6-10 present the typical 32PTH2 DSC temperature distributions for storage conditions. The time-temperature histories for 32PTH2 DSC components during transient blocked vent accident conditions are shown in Figure B.4.6-11.

Figure B.4.6-12 through Figure B.4.6-15 present the typical 32PTH2 DSC temperature distributions for various transfer conditions. The time-temperature histories for 32PTH2 DSC components during transient transfer conditions are shown in Figure B.4.6-16 through Figure B.4.6-18.

The average temperatures for the fuel assemblies and the assembly components are listed in Table B.4.6-18. The average temperatures are used for thermal expansion and DSC internal pressure calculations.

The maximum component temperatures for a 32PTH2 DSC loaded with damaged fuel assemblies resulting from the sensitivity analysis described in Section B.4.6.8 for the loss of neutron shield with loss of air circulation accident condition (Load Case T9 with 16 damaged fuel assemblies) are compared to the corresponding values for the 32PTH2 DSC with intact only fuel assemblies in Table B.4.6-19.

As seen in Table B.4.6-19, the maximum fuel cladding temperature is 900°F for a 32PTH2 DSC loaded with damaged fuel assemblies wherein thermal conductivity of rubble is conservatively considered as helium conductivity. This corresponds to a temperature increase of 13°F when compared to the maximum fuel cladding temperature for the 32PTH2 DSC loaded with intact fuel for Load Case T9. Therefore, considering the large margin of 158°F for the maximum fuel cladding temperature to the accident limit of 1058°F [B4.3], this change does not affect the thermal performance of the 32PTH2 DSC.

Typical component temperature plots for a 32PTH2 DSC with 16 damaged fuel assemblies for the loss of neutron shield with loss of air circulation accident condition are shown in Figure B.4.6-19.

### B.4.6.10 Maximum Internal Pressures for the 32PTH2 DSC

Maximum internal pressure within the 32PTH2 DSC is calculated in Section B.4.7. A summary of the maximum operating pressures for the 32PTH2 DSC is presented in Table B.4.7-1.

### B.4.6.11 Evaluation of 32PTH2 DSC Thermal Performance

As presented in Table B.4.6-14 and Table B.4.6-15, the maximum fuel cladding temperatures are below the allowable fuel temperature limit of 752°F (400°C) [B4.3] for normal storage and normal/off-normal transfer conditions. The 50% blockage of the ASHM-HS inlet vents are considered as an off-normal condition.

The complete blockage of the AHSM-HS inlet and outlet vents during storage and the loss of liquid neutron shield in combination with failure of the air circulation during transfer are considered as accident conditions. As shown in Table B.4.6-14 and Table B.4.6-15, the maximum fuel cladding temperatures remain well below the allowable fuel temperature limit of 1058°F (570°C) [B4.3] for off-normal storage and accident conditions.

The time limits required for transfer operation to maintain the fuel cladding temperature below the allowable limits are discussed in Section B.4.5 and summarized in Figure B.4.5-10.

As presented in Table B.4.7-1, the maximum 32PTH2 DSC internal pressures for normal, off-normal, and accident conditions are 9.4 psig, 18.2 psig, and 124 psig, respectively. These values are calculated based on bounding transfer and storage conditions as documented in Section B.4.7. The calculated DSC internal pressures are lower than the design pressure limits of 15 psig for normal, 20 psig for off-normal, and 140 psig for accident storage and transfer conditions. Hence, the NUHOMS® 32PTH2 DSC design meets all applicable thermal requirements for normal, off-normal, and accident conditions.

**Table B.4.6-15**
**Maximum Fuel Cladding Temperatures for Transfer Conditions**

| Load Case No.[1] | Load Case Description | Time (hr)[3] | Fuel Cladding (°F) | Limit (°F) [B4.3] |
|---|---|---|---|---|
| T1[2] | Normal Hot Transfer, Horizontal, 32.0 kW (HLZC#3) | ∞ | <730 | 752 |
| T2[2] | Normal Cold Transfer, Horizontal, 32.0 kW (HLZC#3) | ∞ | <730 | |
| T3 | Off-Normal Hot Transfer, Horizontal, 32.0 kW (HLZC#3) | ∞[4] | 730 | |
| T4[2] | Off-Normal Cold Transfer, Horizontal, 32.0 kW (HLZC#3) | ∞ | <730 | |
| T5A | Normal Hot Transfer, Vertical, 31.2 kW (HLZC#4) | ∞ | 725 | |
| T5 | Normal Hot Transfer, Vertical Transient, 32.0 kW (HLZC#3) | 75 | 718 | |
| T6 | Normal Hot Transfer, Vertical Transient, 37.2 kW (HLZC#1) | 36 | 715 | |
| T7 | Off-Normal Hot Transfer, Horizontal Transient, 37.2 kW (HLZC#1) | 36 | 711 | |
| T8 | Off-Normal Hot Transfer, Horizontal, Air Circulation, 37.2 kW (HLZC#1) | ∞ | *711* | |
| T9 | Accident, Loss of Neutron Shield with Loss of Air Circulation, 37.2 kW (HLZC#1) | ∞ | 887 | 1058 |
| T10 | Off-Normal, Air Circulation turned-off for off-loading DSC to AHSM-HS or Air Circulation Failure during Transfer Operation, 37.2 kW (HLZC#1) | 12 | *727* | 752 |
| T11 | Normal Hot, Vertical, Initial Conditions, 37.2 kW (HLZC#1) | ∞ | 572 | |
| T12 | Normal Hot, Vertical Steady-State, Initial Conditions, 32.0 kW (HLZC#3) | ∞ | 540 | |

(1) See Table B.4.5-1 for detail descriptions of load cases.

(2) The results for normal hot, cold and off-normal cold transfer conditions (Load Cases T1, T2 and T4) are bounded by the results for hot off-normal storage condition (Load Case T3).

(3) Symbol of "∞" indicates a steady-state analysis.

(4) Although Load Case T3 is analyzed for steady-state conditions, a time limit of 75 hours is selected for transfer operations of the 32PTH2 DSC in the OS200FC TC with heat loads > 31.2 kW and ≤ 32.0 kW (HLZC #3) for conservatism.

**Table B.4.6-17**
**Maximum 32PTH2 DSC Component Temperatures for Transfer Conditions**

| Load Case No.[1] | Time (hr)[3] | Fuel Compartment (°F) | Transition Rails (°F) | Top Shield Plug (°F) | Bottom Shield Plug (°F) | DSC Shell (°F) |
|---|---|---|---|---|---|---|
| T1[2] | ∞ | <700 | <529 | <431 | <441 | <473 |
| T2[2] | ∞ | <700 | <529 | <431 | <441 | <473 |
| T3 | ∞[4] | 700 | 529 | 431 | 441 | 473 |
| T4[2] | ∞ | <700 | <529 | <431 | <441 | <473 |
| T5A | ∞ | 702 | 529 | 456 | 469 | 467 |
| T5 | 75 | 691 | 509 | 416 | 429 | 449 |
| T6 | 36 | 694 | 504 | 377 | 387 | 441 |
| T7 | 36 | 683 | 506 | 367 | 375 | 449 |
| T8 | ∞ | *685* | *490* | *297* | *233* | *408* |
| T9 | ∞ | 869 | 676 | 552 | 564 | 615 |
| T10 | 12 | *704* | *523* | 400 | 321 | *445* |
| T11 | ∞ | 540 | 311 | 282 | 264 | 262 |
| T12 | ∞ | 498 | 296 | 272 | 256 | 254 |

(1) See Table B.4.5-1 for detail descriptions of load cases.

(2) The results for normal hot, cold and off-normal cold transfer conditions (Load Case T1, T2 and T4,) are bounded by the results for hot off-normal storage condition (Load Case T3).

(3) Symbol of "∞" indicates a steady-state analysis.

(4) Although Load Case T3 is analyzed for steady-state conditions, a time limit of 75 hours is selected for transfer operations of the 32PTH2 DSC in the OS200FC TC with heat loads > 31.2 kW and ≤ 32.0 kW (HLZC #3) for conservatism.

**Table B.4.6-18**
**Average Temperatures of 32PTH2 DSC Components for Storage and Transfer Conditions**

| Component | | | | | Hottest DSC Section [5] | | | |
|---|---|---|---|---|---|---|---|---|
| Load Case No.[1] | Time (hr)[4] | Fuel Assembly (°F) | Cavity Gas (°F) | DSC Shell (°F) | Fuel Compartment (°F) | R90 Transition Rail @ 180° (°F) | R90 Transition Rail @ 0° (°F) | DSC Shell (°F) |
| S1 [2] | ∞ | <586 | <426 | <387 | <593 | <462 | <471 | <409 |
| S2 [2] | ∞ | <586 | <426 | <387 | <593 | <462 | <471 | <409 |
| S3 | ∞ | 586 | 426 | 387 | 593 | 462 | 471 | 409 |
| S3A | ∞ | 590 | 430 | 390 | 597 | 464 | 475 | 412 |
| S4 | ∞ | 565 | 413 | 376 | 571 | 448 | 456 | 397 |
| S5 | ∞ | 531 | 392 | 357 | 535 | 424 | 432 | 377 |
| S5A | ∞ | 521 | 386 | 353 | 524 | 418 | 426 | 372 |
| S6 | ∞ | 467 | 294 | 249 | 470 | 339 | 337 | 273 |
| S7 | 40 | 726 | 571 | 552 | 742 | 612 | 638 | 589 |
| T1[3] | ∞ | <594 | <474 | <430 | <598 | <448 | <515 | <443 |
| T2[3] | ∞ | <594 | <474 | <430 | <598 | <448 | <515 | <443 |
| T3 | ∞ | 594 | 474 | 430 | 598 | 448 | 515 | 443 |
| T4[3] | ∞ | <594 | <474 | <430 | <598 | <448 | <515 | <443 |
| T5A | ∞ | 609 | 496 | 454 | 612 | 512 | 512 | 465 |
| T5 | 75 | 590 | 471 | 433 | 594 | 492 | 492 | 446 |
| T6 | 36 | 591 | 454 | 421 | 597 | 484 | 484 | 438 |
| T7 | 36 | 577 | 438 | 402 | 583 | 423 | 489 | 419 |
| T8 | ∞ | *546* | *303* | *295* | *566* | *440*[6] | *440*[6] | *346* |
| T9 | ∞ | 751 | 613 | 571 | 764 | 616 | 658 | 597 |
| T10 | 12 | 580 | 450 | 405 | *604* | *464* | *502* | *425* |
| T11 | ∞ | 429 | 286 | 215 | 423 | 286 | 286 | 213 |
| T12 | ∞ | 397 | 275 | 215 | 391 | 276 | 276 | 213 |

(1) See Table B.4.4-1 and Table B.4.5-1 for a description of the load cases.
(2) The results for hot and cold normal storage conditions (Load Cases S1 and S2) are bounded by the results for hot off-normal storage condition (Load Case S3).
(3) The results for hot and cold normal storage conditions (Load Cases S1 and S2) are bounded by the results for hot off-normal storage condition (Load Case S3).
(4) Symbol of "∞" indicates a steady-state analysis.
(5) Average values are based on the hottest 32PTH2 DSC cross section at the maximum fuel cladding temperature.
*(6) The average of all rails at the hottest cross section is considered.*

*Table B.4.6-22*
*Discretization Error of the 32PTH2 DSC Finite Element Model*

| | Uncertainty in Maximum Fuel Cladding | |
|---|---|---|
| | Set # 1 (Grid # 1, 2, 3) | Set # 2 (Grid # 2, 3, 4) |
| $N_1$ | 1267792 | 2981768 |
| $N_2$ | 468732 | 1267792 |
| $N_3$ | 223080 | 468732 |
| $h_1$ | 0.67 | 0.5 |
| $h_2$ | 0.93 | 0.67 |
| $h_3$ | 1.19 | 0.93 |
| $r_{21}$ | 1.39 | 1.34 |
| $r_{32}$ | 1.28 | 1.39 |
| $\Phi_1$ (°F) | 727.11 | 729.30 |
| $\Phi_2$ (°F) | 721.94 | 727.11 |
| $\Phi_3$ (°F) | 714.76 | 721.94 |
| $\Phi_{Avg}$ (°F) | 721.27 | 726.12 |
| $\varepsilon_{21} = \Phi_2 - \Phi_1$ | -5.17 | -2.19 |
| $\varepsilon_{32} = \Phi_3 - \Phi_2$ | -7.18 | -5.17 |
| $p$ | 2.17 | 2.39 |
| $\Phi^{21}_{ext}$ (°F) | 732.10 | 731.46 |
| $e^{21}_{a}$ | 5.17 | 2.19 |
| $F_s$ | 1.25 | 1.25 |
| $GCI^{21}_{Fine}$ | 6.24 | 2.70 |
| $U_{num}$ (°F) | 6.24 | 2.70 |

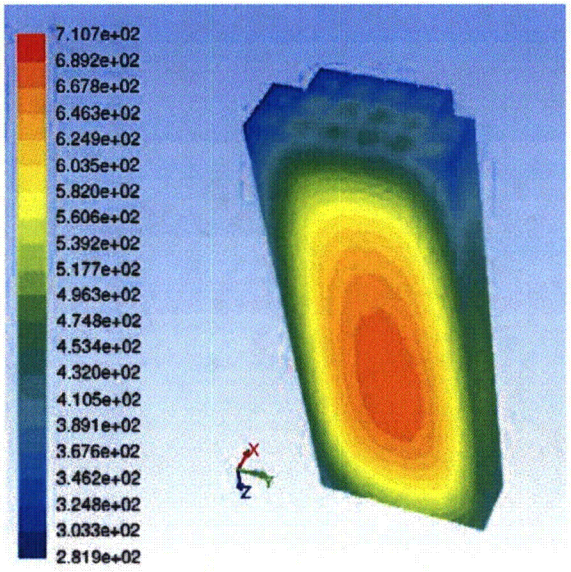


*Fuel Cladding*

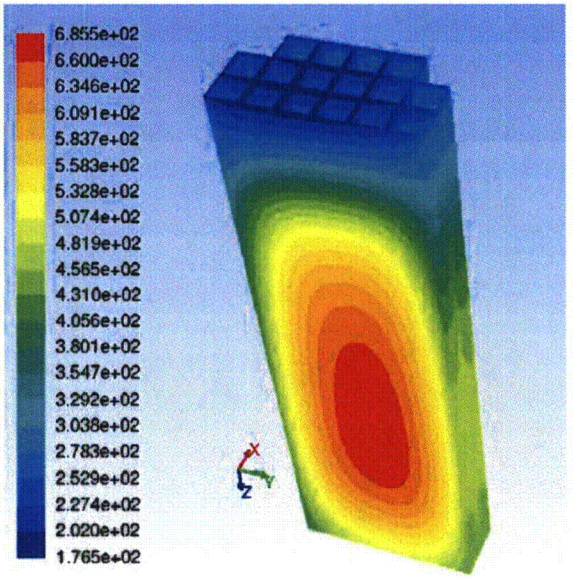


*Fuel Compartment*

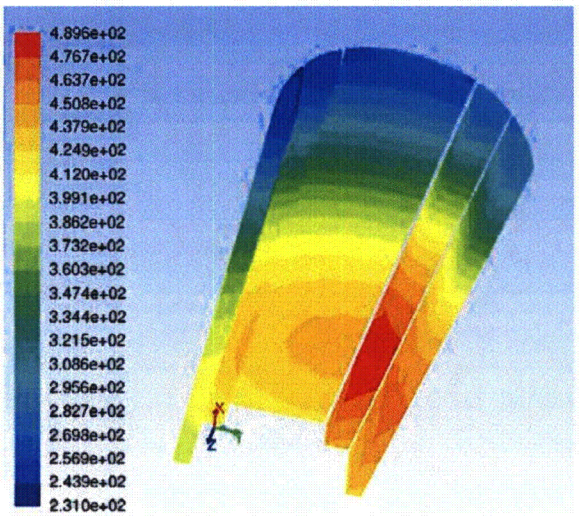


*Basket Rail*

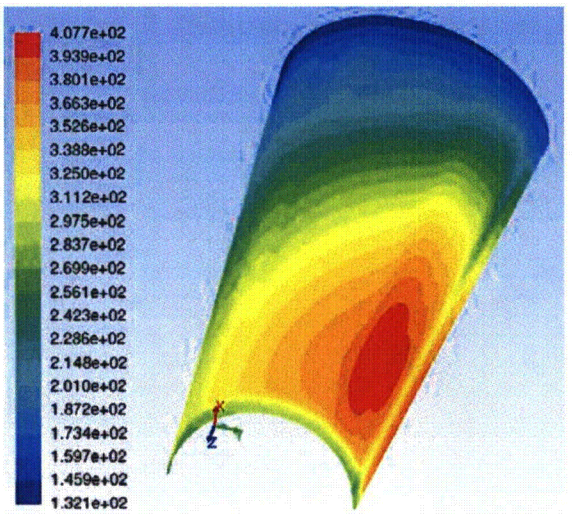


*DSC Cylindrical Shell*

**Figure B.4.6-14**
**Temperature Distribution for 32PTH2 DSC with 37.2 kW in OS200FC TC, with Air Circulation, Off-Normal Hot, Horizontal Steady-State Operations (Load Case T8)**

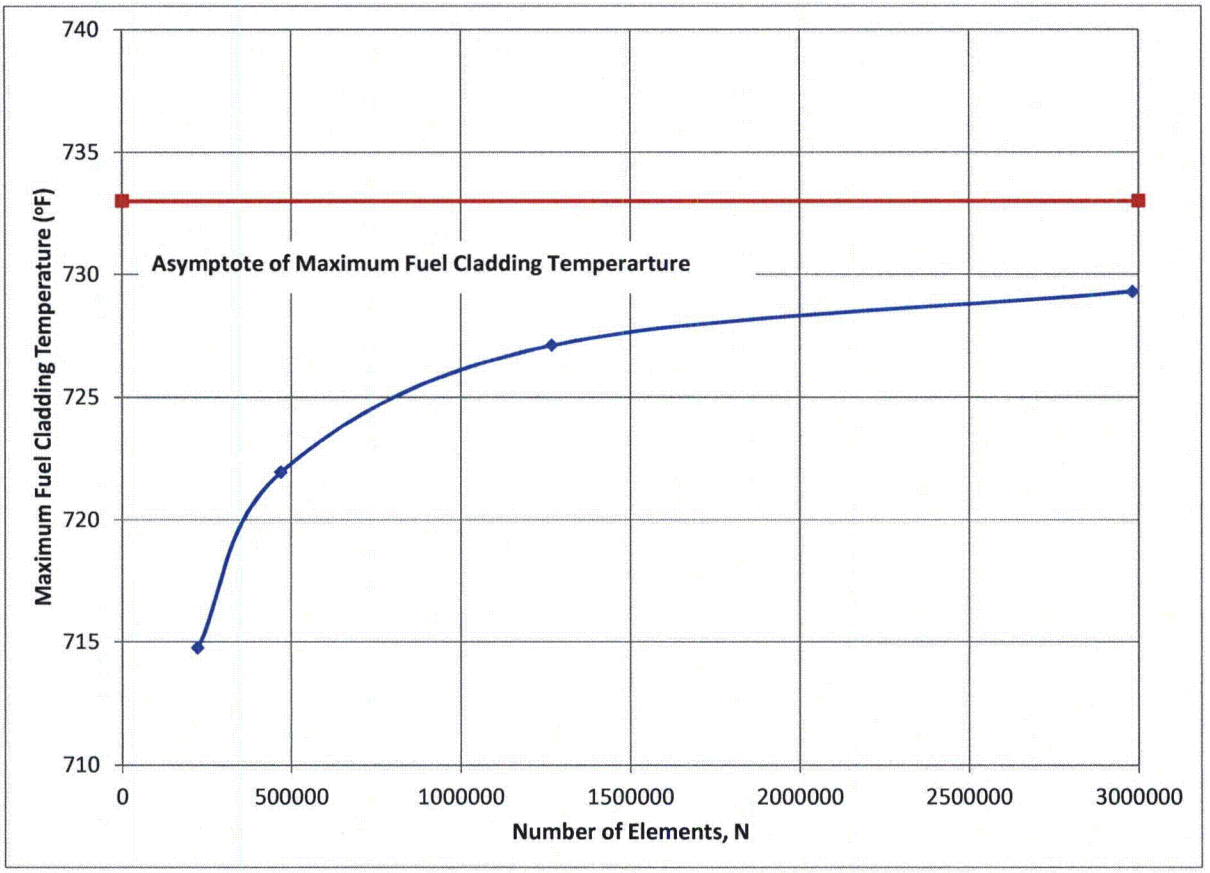


***Figure B.4.6-20***
***Maximum Fuel Cladding Temperature vs. Number of Elements***

[B4.16] Paloposki and Leidquist, Steel Emissivity for Higher Temperatures, Nordic Innovation Centre, NT Technical Report #570, 2006.

[B4.17] Henninger, J. H., "Solar Absorptance and Thermal Emittance of Some Common Spacecraft Thermal-Control Coatings," NASA Scientific and Technical Information Branch, NASA Reference Publication 1121, 1984.

[B4.18] Kreith, Frank, Principles of Heat Transfer, 3rd Edition, 1973.

[B4.19] Amaya, M. et al., Thermal Conductivities of Irradiated UO2 and (U,Gd)O2, Journal of Nuclear Materials 300 (2002) 57–64.

[B4.20] Ronchi, et. al., Effect of Burn-up on the Thermal Conductivity of Uranium Dioxide up to 100,000 MWd/t, Journal of Nuclear Materials, 327 (2004) 58-76.

[B4.21] GESC, NAC International, Atlanta Corporate Headquarters, 655 Engineering Drive, Norcross, Georgia, (Engineering Report #NS3-020, Effects of 1300°F on Unfilled NS-3, while Bisco Products, Inc., 11/84).

[B4.22] Transnuclear, Inc., Updated Final Safety Analysis Report for the Standardized NUHOMS® Horizontal Modular Storage System for Irradiated Nuclear Fuel, Revision 11, USNRC Docket No. 72-1004.

[B4.23] *ANSYS FLUENT computer code, Version 14.0*.

[B4.24] Transnuclear, Inc., Safety Analysis Report for the NUHOMS®-MP197 Transport Packaging, Chapter A.3, USNRC Docket No. 71-9302, Revision 10, ML11238A106.

[B4.25] Transnuclear, Inc., Report, Thermal Testing of the NUHOMS® Horizontal Storage Module, Model HSM-H, Report No. E-21625, Revision 1, ML050680050.

[B4.26] ANSYS computer code and On-Line User's Manuals, Version 10.0.

[B4.27] U.S. Nuclear Regulatory Commission, Final Safety Evaluation Report, Transnuclear, Inc., Standardized NUHOMS® Horizontal Modular Storage System for Irradiated Nuclear Fuel, Docket No. 72-1004, Amendment No. 10, ML092290329.

[B4.28] American Concrete Institute, Code Requirements for Nuclear Safety Related Concrete Structures (ACI 349-97) and Commentary (ACI 349R-97), 1997.

[B4.29] GESC NS-3, NAC International, Atlanta Corporate Headquarters, 655 Engineering Drive, Norcross, Georgia (Test Report NS-3-001, while Bisco Products, Inc.).

[B4.30] Transnuclear, Inc., Updated Final Safety Analysis Report for NUHOMS® HD Horizontal Modular Storage System for Irradiated Nuclear Fuel, Revision 2.

[B4.31] Oak Ridge National Laboratory, RSIC Computer Code Collection, "SCALE, A Modular Code System for Performing Standardized Computer Analyses for Licensing Evaluation," NUREG/CR-0200, Revision 1, ORNL/NUREG/CSD-2/V3/R6, May 2010.

[B4.32] Oak Ridge National Laboratory, Thermo-physical Properties of MOX and UO2 Fuels Including the Effect of Irradiation, by S.G. Popov, J.J. Carbajo, V. K. Ivanov, G.L. Yoder, ORNL/TM-2000-351, November 2000.

*[B4.33] American Society of Mechanical Engineers, "Standard for Verification and Validation in Computational Fluid Dynamics and Heat Transfer," ASME V&V 20-2009, November 30, 2009.*

*[B4.34] Fundamental FEA Concepts and Applications, ANSYS Inc.*

*[B4.35] Examining Spatial (Grid) Convergence, NPARC Alliance CFD Verification and Validation Website, http://www.grc.nasa.gov/WWW/wind/valid/tutorial/spatconv.html.*

*[B4.36] Ismail B. Celik et.al, "Procedure for Estimation and Reporting of Uncertainty Due to Discretization in CFD Applications", Journal of Fluids Engineering, ASME, July 2008, Vol. 130.*